



Cite this: DOI: 10.1039/d5cc04691b

Molecular organic solid-state electrolytes (MOSSEs): a review of an overlooked class of solid electrolytes

Halil Al-Salih, Zouina Karkar and Yaser Abu-Lebdeh*

Lithium-ion batteries are crucial for applications like consumer electronics, electric vehicles, and renewable energy storage. Despite their importance, challenges persist in enhancing electrode materials for higher energy density, faster kinetics, and cycle life. Improving the safety and reliability of electrolytes is also vital, as traditional liquid electrolytes pose flammability and leakage risks. While carbonate-based liquid electrolytes are commonly used, they face limitations such as narrow electrochemical stability windows and compatibility issues with high-capacity or high-voltage electrodes. Solid electrolytes offer a promising alternative, providing improved safety and enabling the use of lithium metal anodes for higher energy density. The main types are solid polymer electrolytes (SPEs), inorganic solid electrolytes (ISEs), and their composites. This review introduces and examines molecular organic solid-state electrolytes (MOSSEs), a sub-class of molecular solid electrolytes (MSEs) formed by combining salts of alkali metal cations (e.g., Li^+ , Na^+ and K^+) with weakly coordinating organic molecules. These systems give rise to solids with unique crystalline structures that exhibit high ionic conductivity reaching $10^{-3} \text{ S cm}^{-1}$ at ambient temperatures. MOSSEs also possess a low Young's modulus, improving electrode–electrolyte contact and lowering interfacial resistance, while facilitating processing and cell fabrication. We analyze the synthesis methods, structural characteristics, ion transport mechanisms, electrochemical stability windows, and battery performance of various MOSSE systems. Challenges such as moderate thermal stability and limited scalability are addressed, alongside strategies to improve interfacial compatibility and expansion of their electrochemical stability window. By overcoming key limitations of conventional solid electrolytes, such as brittleness, poor electrode–electrolyte contact, and high-temperature processing, MOSSEs offer a promising path toward safer, high-performance solid-state batteries for lithium and beyond-lithium systems.

Received 15th August 2025,
Accepted 26th November 2025

DOI: 10.1039/d5cc04691b

rsc.li/chemcomm

Introduction

The growing demand for high-performance energy storage systems in consumer electronics, electric vehicles, and renewable energy applications continues to push the limits of lithium-ion battery technology. As society increasingly relies on portable and sustainable energy sources, enhancing the capabilities of lithium-ion batteries becomes paramount. To meet these increasing demands, researchers are exploring new approaches to improve battery safety, efficiency, and capacity.

While liquid electrolytes based on organic carbonates have been the industry standard, their inherent safety risks and limited thermal stability have driven the search for safer alternatives. The flammability of organic solvents and the potential

for leakage pose significant safety hazards, including fire and explosion risks.¹ Solid-state electrolytes (SSEs) are emerging as a promising solution to these challenges, offering the potential to eliminate flammable liquid components and support the use of high-energy-density lithium metal anodes.^{2–5}

With their highest theoretical capacity ($\approx 3860 \text{ mAh g}^{-1}$) and lowest electrochemical potential, lithium metal anodes could significantly enhance the energy density of batteries.⁶ However, integrating these anodes requires solid electrolytes that can provide both stable interfaces and efficient ion transport. Solid electrolytes must effectively suppress dendrite formation, which can lead to short circuits and battery failure.⁷ In this context, two main classes of solid electrolytes have gained attention: inorganic ceramics and organic polymers.

Inorganic ceramic electrolytes, such as oxides and sulfides, are known for their electrochemical stability and high ionic conductivity. Materials like garnet-type $\text{Li}_7\text{La}_3\text{Zr}_2\text{O}_{12}$ (LLZO), phosphates $\text{Li}_{1.3}\text{Al}_{0.3}\text{Ti}_{1.7}(\text{PO}_4)_3$ (LATP)/thiophosphate

Energy, Mining, and Environment Research Centre, National Research Council of Canada, 1200 Montreal Road, Ottawa, Ontario K1A 0R6, Canada.
E-mail: Yaser.Abu-Lebdeh@nrc-cnrc.gc.ca



$\text{Li}_{10}\text{GeP}_2\text{S}_{12}$ (LGPS), sulphides (argyrodites or $\text{Li}_2\text{S-P}_2\text{S}_5$ -based) and halides (LiInCl_4) exhibit conductivities comparable to liquid electrolytes.^{8,9} Yet, these materials still face challenges related to brittleness, high interfacial resistance, and complex processing requirements.¹⁰ The rigidity of ceramics leads to



Hilal Al-Salih

Dr Hilal Al-Salih is a Research Officer with the Battery Materials Innovation Team at the National Research Council of Canada (NRC) in Ottawa. His research focuses on advanced solid and liquid electrolyte systems, composite electrode architectures, interfacial stability, and theoretical modeling of ion transport in concentrated electrolyte environments. He also investigates the relationship between electrolyte thermodynamics, conductivity, and

phase behavior, with emphasis on designing materials that enable safe and high-performance lithium batteries and beyond. Dr Al-Salih received his Bachelor's degree in Chemical Engineering from the American University of Sharjah in 2018 and earned his PhD in Chemical Engineering from the University of Ottawa in 2023.



Zouina Karkar

Dr Zouina Karkar is a Research Officer with the Battery Materials Innovation Team at the National Research Council of Canada (NRC) in Ottawa. Her research focuses on surface science and the design and manufacturing of advanced materials for electrochemical energy storage, including cathode and solid-electrolyte materials, as well as surface functionalization strategies to stabilize interfaces in lithium-ion batteries. She received her BS

and MS degrees from the University of Clermont-Ferrand (France) and completed a joint PhD in Materials Science at the University of Nantes (France) and INRS (Canada), with work dedicated to the development of silicon electrodes for Li-ion batteries. Dr Karkar previously worked at the National Center in Environmental Technology and Electrochemistry (CNETE, Canada), where she contributed to projects on lithium hydroxide production via membrane electrodialysis, battery recycling, and scalable, environmentally friendly electrochemical processes for graphite exfoliation.

poor contact with electrode materials, and their sensitivity to moisture complicates manufacturing and handling.¹¹

On the other hand, polymer-based solid electrolytes are more flexible and cost-effective, but their ionic conductivity often falls short. Polyethylene oxide (PEO)-based electrolytes, for instance, require elevated temperatures to achieve adequate ionic conductivity due to the crystalline nature of PEO at room temperature.^{12,13} Additionally, many polymer electrolytes, including PEO, exhibit limited electrochemical stability windows, especially under high-voltage operation (<3.5 V), which constrains their compatibility with next-generation cathodes.¹² Recent efforts have focused on overcoming these limitations by exploring hybrid and composite electrolyte systems,^{13–19} as well as new material classes like sulfides, halides, and argyrodite-type compounds. Composite electrolytes aim to combine the high conductivity of ceramics with the flexibility of polymers, but achieving a homogeneous mixture and good interfacial contact remains challenging.²⁰

An overlooked group of solid electrolytes, often not properly classified, is molecular solid electrolytes (MSEs), which consist of solid materials formed from salts and molecular organic compounds. Within this class, we introduce a distinct sub-category termed molecular organic solid-state electrolytes (MOSSEs), comprising crystalline materials formed by combining alkali metal salts with weakly coordinating organic molecules. MOSSEs offer a unique structure for fast ion migration exhibiting mechanically soft yet crystalline character. We refer



Yaser Abu-Lebdeh

Dr Abu-Lebdeh is a Senior Research Officer and Leader of the Battery Materials Innovation Team at the National Research Council of Canada in Ottawa. His research focuses on electrochemical energy storage and conversion materials and devices, with focus on lithium batteries. Dr Abu-Lebdeh earned his PhD in Electrochemistry from the University of Southampton (UK) in 2001, his Master's degree in Materials Science from the University of Manchester (UK) in 1997 and his bachelor's degree in Industrial Chemistry from Jordan University of Science and Technology in 1995. He joined the NRC in 2005 as an NSERC Postdoctoral Fellow and before that he was a Postdoctoral Research Fellow at the University of Montreal's International Laboratory on Electro-active Materials. He contributed to more than 120 technical reports, peer-reviewed publications and patents and co-edited a book on Nanotechnology for Lithium-ion batteries. Dr Abu-Lebdeh is also an adjunct professor at the University of Toronto's Materials Science and Engineering Department and a part-time professor at the University of Ottawa teaching a course on Battery Technology. Dr Abu-Lebdeh is the recipient of the 2025 Killam NRC Paul Corkum Fellowship.



to these as “soft cocrystals”, a term that reflects their solid-state crystalline nature formed by co-crystallized salt and solvent, along with their inherently low rigidity and cohesive energy, in contrast to dense ceramic lattices. The ion conduction channels in these cocrystals consist of weak Lewis basic donor groups from the organic molecules, enabling flexible yet efficient ion transport pathways. This structural difference potentially overcomes several limitations of traditional inorganic solid electrolytes, including interfacial brittleness and high processing temperatures.²¹ Fig. 1 presents what we consider a completed SSE classification tree diagram without omitting the usually overlooked molecular class of SSEs. The relative strengths and weaknesses of MOSSEs compared to other electrolyte classes are summarized in Fig. 2, which highlights their balanced performance in ionic conductivity, interfacial compatibility, and mechanical compliance.

Crystalline molecular organic materials, which include many MOSSEs, are generally characterized as mechanically soft solids composed of a three-dimensional periodic arrangement of organic molecules. Their cohesion arises primarily from weak intermolecular interactions, such as dipole–dipole forces, hydrogen bonding, and π – π stacking, rather than strong covalent or ionic bonds. This inherently loose packing gives rise to structural features analogous to those found in plastic crystals, including a high density of slip planes. These planes facilitate the formation and motion of dislocations under mechanical stress, enabling plastic deformation without fracture. As a result, MOSSEs exhibit low Young's modulus and favorable interfacial compliance, making them well-suited for solid-state battery applications where soft mechanical contact with electrodes and resistance to cracking are critical.²² Besides, their simple preparation through low temperature solvent or melt casting will allow for ease of processing, scale up and cell fabrication. However, this mechanical softness also introduces

concerns regarding structural fragility, dendrite penetration under high current densities, and insufficient resistance to compressive or puncture forces. These factors can compromise cycle life and interfacial stability, and must be carefully addressed through composite design or interface engineering.

Compared to conventional solid polymer electrolytes, such as the PEO-based systems discussed earlier, MOSSEs can exhibit high ionic conductivity at room temperature due to their unique crystal structures facilitating ion movement.²³ Unlike conventional solid-state electrolytes, which are often limited by either mechanical rigidity (like ISEs with ceramic nature) or low ionic conductivity (like SPES), MOSSEs represent a unique class of materials that combine the mechanical flexibility of organic molecules with the ionic conductivity of inorganic salts. Fig. 3 provides a comparative analysis of MOSSEs within the broader context of electrolyte materials. As shown in Fig. 3a, representative MOSSEs, such as 5 wt% with lithium bis(trifluoromethanesulfonyl)imide (LiTFSI) in succinonitrile, exhibit ionic conductivities approaching those of gel and organic liquid electrolytes while maintaining a solid-state form. This highlights their potential to outperform conventional polymer electrolytes (*e.g.*, LiClO₄) under ambient conditions. In Fig. 3b, a simplified binary phase diagram illustrates the thermodynamic origins of two key MOSSE categories: eutectic MOSSEs, which occur at minimum-melting compositions, and solvate MOSSEs, which form at fixed salt–solvent ratios resulting in ordered crystal lattices. These structural archetypes influence both ion transport and stability, serving as a design framework for developing high-performance MOSSEs.

MOSSEs stand out for their ability to merge the advantageous properties of both solid and liquid electrolytes, including improved ionic conductivity, excellent mechanical properties, and enhanced safety due to their non-volatile nature. Their

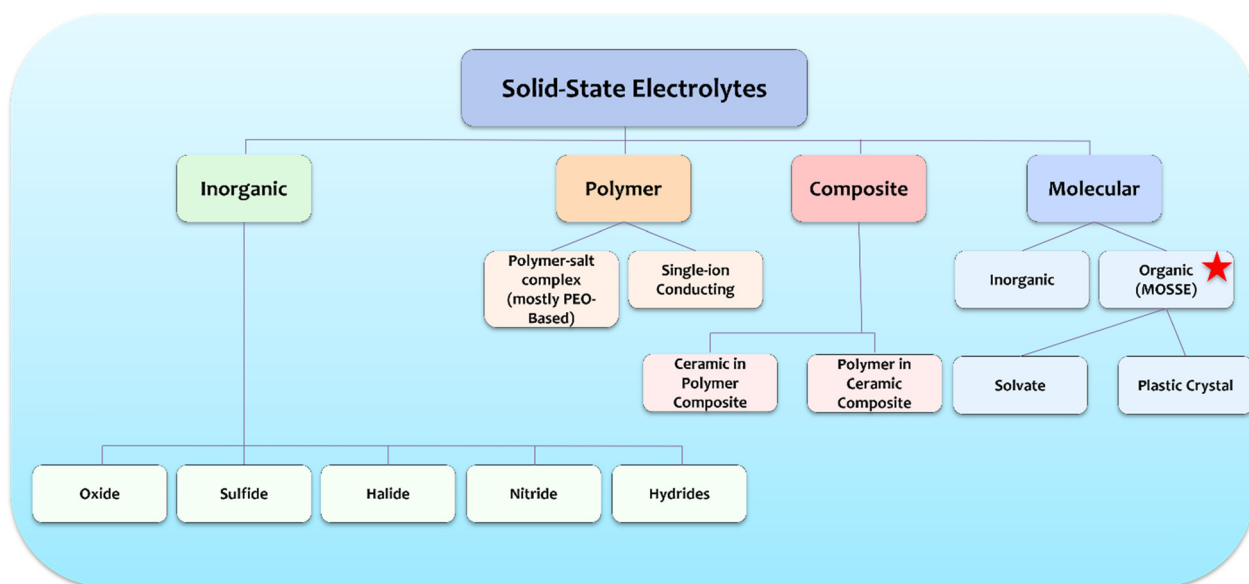


Fig. 1 Tree diagram showing SSE classification including MOSSE, the usually overlooked class.



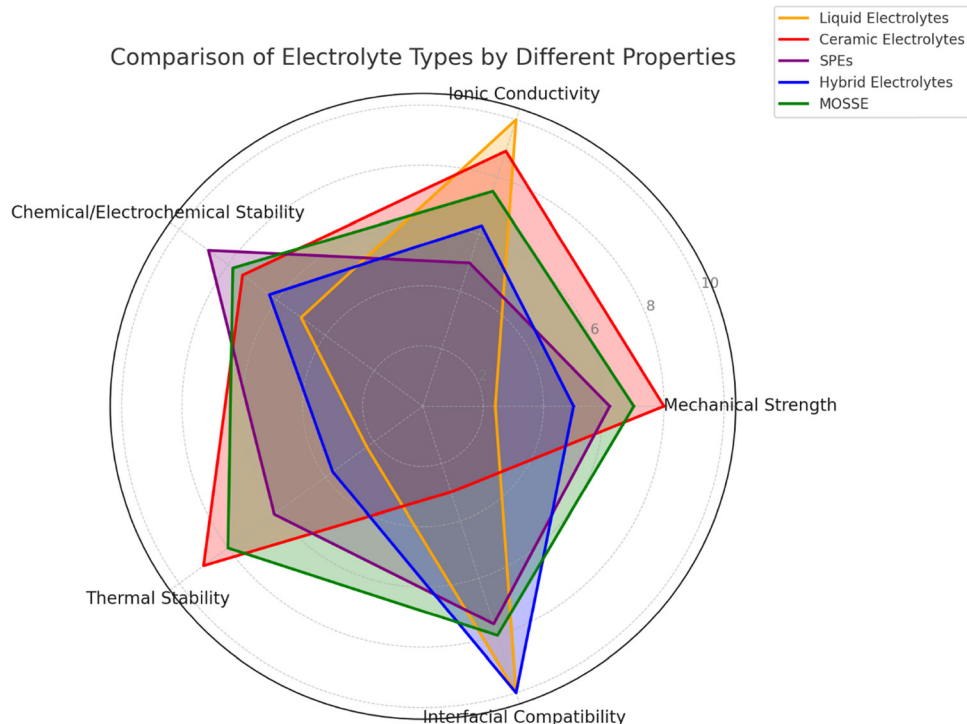


Fig. 2 Radar chart depicting strength and weaknesses of each SSE class.

crystalline nature provides structural stability, while the organic components offer flexibility and processability.²⁴ This innovative approach opens up new possibilities for developing solid-state batteries that can overcome the limitations of traditional liquid and polymer electrolytes. By leveraging the unique structural characteristics of MOSSEs, researchers are exploring their potential to enable the use of lithium metal anodes, thereby pushing the boundaries of energy density and battery performance.

Building on the Pearson hard–soft acid–base (HSAB) theory, researchers hypothesized that the conductivity of soft solid electrolytes could be enhanced by using a soft donor solvent matrix with which the hard Li^+ ions interact weakly. According to the HSAB theory, “hard” acids like Li^+ prefer to bind with “hard” bases, but by introducing “soft” bases, the interaction is weakened, facilitating ion mobility.²⁵ This hypothesis led to the exploration of various solvent and salt composite materials, such as salts complexed in succinonitrile (SN), adiponitrile (ADN), acetonitrile (AN), ethylene carbonate (EC), propylene carbonate (PC), dimethyl carbonate (DMC), diethyl carbonate (DEC), ethyl methyl carbonate (EMC), ethyl acetate (EA), sulfolane, tetrahydrofuran (THF), dimethylformamide (NN DMF), and 1,2-dimethoxyethane (DME). Fig. 4 illustrates the line structure of these solvent examples.

An important subset of MOSSEs is the solvate MOSSEs, which form when a lithium salt and a molecular solvent are combined at specific stoichiometric ratios, known as solvate compositions, corresponding to distinct points in the phase diagram. At this precise ratio ($x = x_s$), the resulting solid is a well-defined crystalline compound in which solvent molecules

are systematically integrated into the crystal lattice alongside the salt ions. This ordered integration creates stable and uniform microstructures, often exhibiting superior thermal stability, enhanced ionic conductivity, and predictable solubility. At the stoichiometric solvate composition, the MOSSE can also be fabricated *via* a melt-casting process. As shown in Fig. 5, the lithium salt and donor solvent are first combined at the appropriate molar ratio and gently heated above the compound's melting point to form a homogeneous liquid. Upon cooling, the mixture solidifies into a single-phase crystalline MOSSE. Fig. 5a illustrates this melt-casting strategy, while Fig. 5b shows a representative image of the resulting solidified MOSSE, prepared from LiTFSI and DME in a 1:3 molar ratio, demonstrating its pure-phase, glassy morphology in a flipped vial. This visual homogeneity is consistent with the formation of a stoichiometric, solvent-free crystalline electrolyte rather than a metastable or biphasic mixture.

The structural integrity of solvate MOSSEs promotes the formation of ion-conducting channels through aligned solvent molecules, facilitating efficient lithium-ion transport. Additionally, the presence of thermally activated or intrinsic vacancies within the lattice supports ion hopping between coordination sites, further contributing to conductivity. In contrast, off-stoichiometric compositions ($x \neq x_s$) often result in heterogeneous or metastable solids, such as mixtures of salt and excess solvent or solute, that lack the same degree of crystalline order, leading to variable and often inferior electrochemical performance.

Furthermore, the conductive behavior of solvate MOSSEs can be finely tuned by selecting different solvents or counter



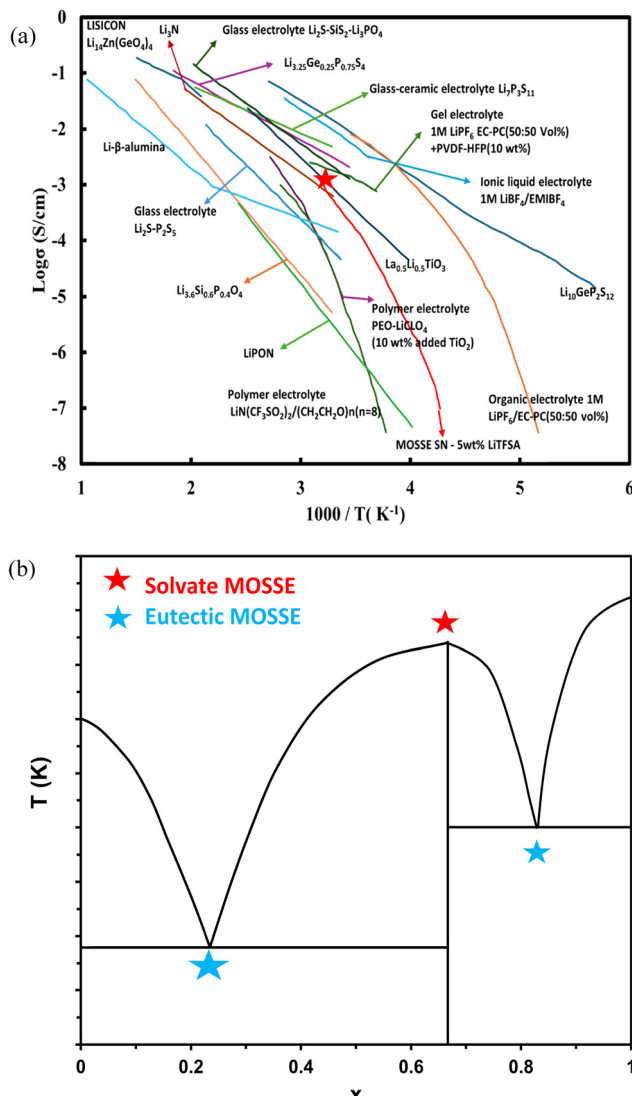


Fig. 3 (a) Comparison of temperature-dependent ionic conductivities ($\log \sigma$ vs. $1000/T$) for various solid and liquid electrolytes, highlighting the position of a representative molecular organic solid-state electrolyte (MOSSE) system (5 wt% LiTFSI in succinonitrile).⁴⁵ The MOSSE exhibits higher conductivity than traditional polymer electrolytes (e.g., PEO- LiClO_4) and approaches values reported for gel and liquid systems, while maintaining a solid-state form (reproduced from ref. 25 with permission from Royal Society of Chemistry, copyright 2025). (b) Schematic phase diagram illustrating eutectic (blue star) and solvate (red star) compositions in binary salt–solvent systems. Eutectic compositions correspond to the minimum in the melting temperature, while solvates correspond to a minimum that occurs at specific stoichiometries with distinct crystalline structures. These two states represent key categories of MOSSEs, each with different thermodynamic and transport characteristics.

anions. Lithium salts coordinated by low-molecular-weight ligands and weakly coordinating anions have demonstrated particularly high conductivities. These characteristics, combined with their structural predictability, make solvate MOSSEs highly promising for next-generation solid-state battery applications. This review aims to provide a comprehensive examination of MOSSEs and their properties. By highlighting the advancements and remaining challenges in this field, the

review seeks to inform future research directions and contribute to the development of more efficient and reliable solid-state lithium metal batteries. We will discuss the synthesis methods, structural characteristics, ion transport mechanisms, and electrochemical performance of various MOSSEs, providing comparative analyzes where applicable.

1. Solvation structures and ionic association in MOSSEs

To build a deeper understanding of how salt–solvent interactions define the structural and transport properties of MOSSEs, it is essential to examine the specific coordination environments and phase behaviors that emerge across different systems. The following sections explore representative solvate MOSSEs formed with various solvents, including dimethyl sulfoxide (DMSO), glymes, and nitriles, highlighting how molecular structure, stoichiometry, and ionic association influence their conductivity, stability, and suitability for solid-state battery applications.

The performance of these electrolytes is heavily influenced by the microstructures formed between lithium salts and polar aprotic solvents. A key example of this interaction can be seen with DMSO, where lithium salts form solvates with the general composition $\text{LiX} \cdot 4\text{DMSO}$ with X being BF_4^- , NO_3^- , or CF_3SO_3^- . Among these solvates, $\text{LiCF}_3\text{SO}_3 \cdot 4\text{DMSO}$ demonstrates the highest stability, followed by $\text{LiBF}_4 \cdot 4\text{DMSO}$ and $\text{LiNO}_3 \cdot 4\text{DMSO}$. This variation in stability is attributed to the differing anion interactions with DMSO. According to Esin's thermodynamic formalism,²⁶ the order of anion association with DMSO follows the trend $\text{ClO}_4^- > \text{CF}_3\text{SO}_3^- > \text{BF}_4^- > \text{NO}_3^-$, with each interaction directly influencing solvate stability and ionic conductivity.²⁶ Unlike solvents such as propylene carbonate (PC) and dimethyl carbonate (DMC), which often form less stable or weakly dissociated complexes with lithium salts, DMSO can strongly coordinate Li^+ and form stable solvates. For example, LiClO_4 in DMSO exhibits significantly higher ionic conductivity, attributed to enhanced ion dissociation and mobility. This reinforces the critical role that salt–solvent interactions play in enhancing the performance of these electrolytes. By carefully selecting and optimizing these interactions, MOSSEs can achieve the necessary balance between stability and ionic conductivity, making them strong candidates for next-generation high-performance battery applications.²⁷

Glymes (G1, G2, G3, G4; short for mono-, di-, tri-, and tetraethylene glycol dimethyl ethers and so on), belonging to the ether-oxide family, interact with lithium salts to form a variety of solvates, each exhibiting distinct ionic association strengths. In dilute solutions, lithium ions are highly solvated, existing as “free” ions, but as the concentration increases, these ions transition into more structured forms, including solvent-separated ion pairs (SSIP), contact ion pairs (CIP), and aggregates (AGG).²⁸ SSIP, CIP, and AGG have an impact on the viscosity, conductivity, and the electrochemical window of the



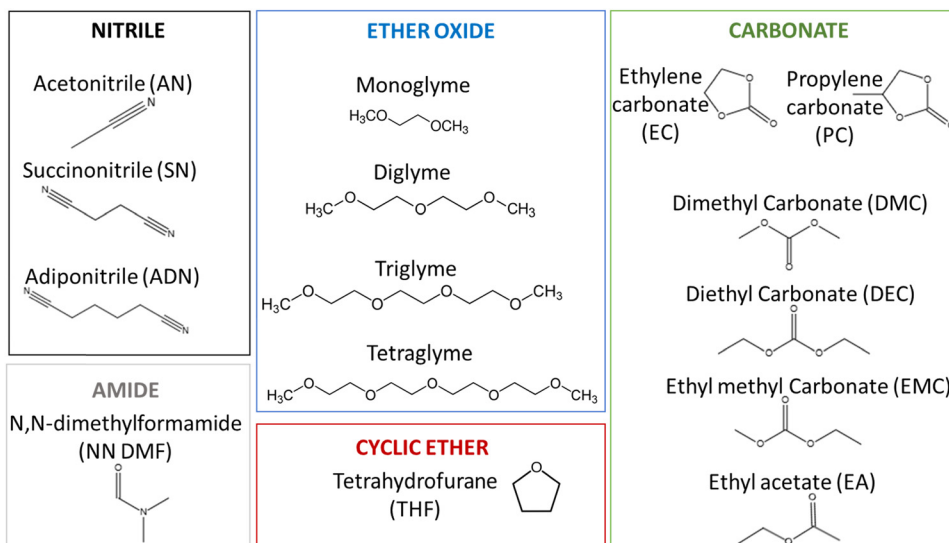


Fig. 4 Representative molecular organic solvents that form co-crystalline solid-state electrolytes (MOSSEs) with lithium salts.

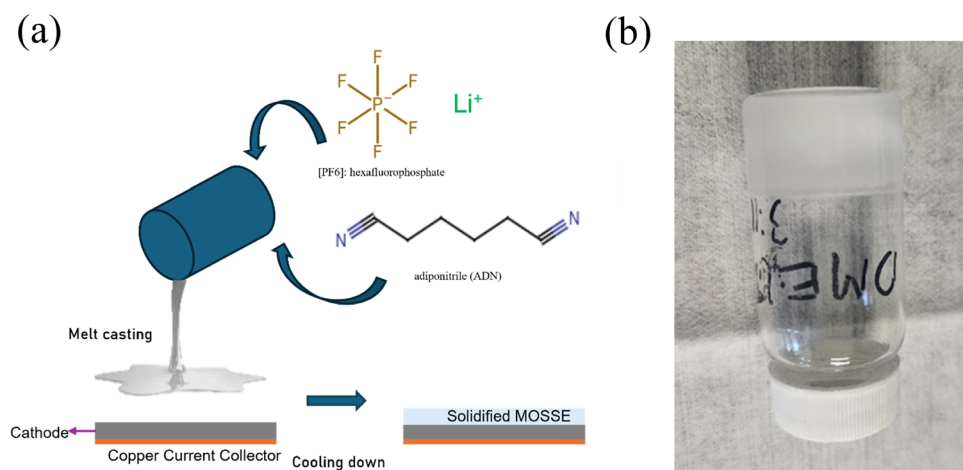


Fig. 5 (a) Schematic of the melt-casting process of MOSSE. (b) Sample image to visualize the non-fluidity of DME–LiTFSI (3:1) solvate MOSSE prepared in our lab using inverted vial method. Sample was prepared by simple mechanical stirring above solvate melting point (29 °C) then left to solidify at room temperature.

electrolyte.^{29–32} The coordination number of lithium cations within these structures typically ranges from 4 to 6, though variations from 3 to 8 are also observed depending on the system. In glymes, lithium salts are categorized by their degree of ionic association, spanning from highly dissociated salts like LiBPh₄ to more strongly associated salts like LiNO₃ and LiCF₃CO₂. At sufficiently high salt concentrations, the coordination of all solvent molecules to Li⁺ ions alters the electronic structure of the electrolyte, often localizing the LUMO on the anion (*e.g.*, TFSI[–]) rather than the solvent. This effect, observed in systems based on glymes, succinonitrile, NN DMF, and acetonitrile, enhances the reductive stability of the solvent by promoting preferential anion reduction and the formation of stable SEI layers.^{33–36}

The stability and melting points of these solvates are closely tied to the strength of ionic association. Higher degrees of

association often result in more complex phases, such as CIP or AGG, which can influence both the mechanical and electrochemical properties of the materials. Additionally, crystallinity gaps composition ranges where no stable crystalline phase forms frequently arise in glyme–LiX mixtures when ionic association is particularly strong or when higher glyme-to-salt ratios are employed. These gaps highlight the challenges in achieving stable crystalline phases under such conditions, which can complicate the design of solid electrolytes based on these systems.³⁷

A detailed analysis of specific solvate structures, such as (G1)_n–LiClO₄ and (G2)_n–LiClO₄ mixtures, reveals significant insights into their thermal properties, crystal structures, and ion association behaviors. The (G1)₂ solvate, for example, melts at 68 °C, where Li⁺ cations are coordinated by four ether oxygen atoms from G1 molecules and two oxygen atoms from a



Table 1 Examples of different MOSSE sub classes, and their key properties

Group	Representative systems	Key strengths/distinctive features (condensed)	Ref.
(1) Glyme-based solvates (ethers-oxide)	$(G1)_3\text{LiTFSI}$, $(G2)_2\text{LiTFSI}$, $(G4)_{0.5}\text{LiBF}_4$, $[\text{Li}(G3)][\text{TFSA}]$, $[\text{Li}(G4)][\text{TFSA}]$, $G4\text{LiAsF}_6$	Stable, stoichiometric MOSSE crystals with well-defined 4–6–38 and coordinate Li^+ environments; persistent solvate species in the 40–44 melt (verified by phase diagrams + Raman); strong chelation suppresses ion pairing; high oxidative stability (~5 V) and fast Li^+ transport <i>via</i> cation–solvent complexes yield conductivities of 10^{-4} – 10^{-3} S cm $^{-1}$	4–38 and 40–44
(2) Nitrile-based solid systems (SN/ADN)	SN + 5 wt% LiTFSI, SN + 5 mol% LiTFSI, SN + 5 wt% LiBF ₄ , (ADN) ₂ LiPF ₆ , (ADN) ₃ NaClO ₄ , (AN) _n LiPF ₆ , 4.2 mol dm $^{-3}$ LiTFSI in AN	Plastic-crystal MOSSEs with rotationally mobile CN framework; strong dielectric screening enabling full salt dissociation; weak Li^+/Na^+ binding promoting low-barrier hopping; 3D ion-transport channels with nanoliquid grain-boundary layers that suppress interfacial resistance; melt-castable, mechanically compliant, and anodically stable up to 5–7 V	23, 24, 39 and 45–49
(3) Amide/Amine-based solvates	LiCl·DMF, NaClO ₄ (DMF) ₃ , LiTFSI-acetamide, Li(TFSA)(Me ₂ NCH ₂ CH ₂ NMe ₂), isoquinoline ₃ ·(LiCl) ₂	Strong C=O and N-donor coordination forming rigid crystalline solids; moderate ionic conductivities (10^{-4} – 10^{-6} S cm $^{-1}$); relatively low activation barriers for Li^+ hopping; several systems exhibit high thermal robustness (>140 °C), suitable for high-temperature solid-state operation	50–56
(4) Aromatic/crown-ether-based solvates	(18-Crown-6)·LiTFSI, 1,2-dimethoxybenzene/LiTFSI, 1,2-F ₂ -DMB/LiTFSI, Li(TFSA)(DMB) _{1–2}	Engineered host-guest Li^+ sites yielding single-ion conduction ($t^+ \approx 0.9$); π -stacked aromatic frameworks creating directional 1D Li^+ hopping paths; TFSA [–] immobilization forming rigid anion networks; transport governed by Li–Li spacing and weakened Li–O chelation; plastic or solid–solid transitions enhancing mobility; stable to ~4 V with demonstrated Li metal cycling	51, 57 and 58
(5) Carbonate/lactone-based solvates	(EC) _{2–3} ·LiClO ₄ , (GBL) _{1–4} ·LiPF ₆ , (GVL) ₁ ·LiClO ₄ , (EC) ₁ ·LiCF ₃ SO ₃	Exclusive carbonyl-O coordination giving uniform 4-coordinate Li^+ sites; packing motifs replicate liquid EC/GBL solvation structures; anion-dependent ion-pairing and aggregation; simple lattices isolating solvent-anion competition; moderate conductivity (10^{-5} – 10^{-4} S cm $^{-1}$)	59
(6) Sulfone/sulfolane-based solvates	LiBF ₄ /SL (1:1), LiTFSA/SL (1:1), KFSI/DMS (1:9)	Strong S=O dipole coordination forming highly stable solvates; wide oxidative stability windows (up to 6.2 V); conductivities of 10^{-4} – 10^{-3} S cm $^{-1}$; excellent high-voltage compatibility and thermal robustness in sulfolane and sulfone systems	60 and 61

bidentate ClO_4^- anion, forming a CIP-II structure. In contrast, the $(G2)_2$ solvate melts at 71 °C and features a six-coordinate Li^+ , bonded to six ether oxygen atoms from G2 molecules, resulting in solvent-separated ion pairs (SSIPs). Vibrational spectroscopy further distinguishes these solvates by identifying shifts in ClO_4^- frequencies, which help differentiate between species.³⁸ Additionally, phase diagrams and conductivity measurements of lithium salt systems in solvents like AN–LiTFSI and AN–LiPF₆ illustrate the variety of solvate structures and their corresponding phase behaviors.

In the case of acetonitrile (AN), a solid–solid phase transition occurs at –56 °C before melting at –46 °C, characterized by a distinctive 90° rotation of AN molecular slabs within the crystal lattice. This transformation significantly impacts the solid phase's structure and its interaction with lithium salts. When AN is mixed with LiTFSI, the phase behavior becomes more complex. The 6/1 and 4/1 molar ratio solvates display differing coordination environments, and Li^+ cations in the 6/1 phase are octahedrally coordinated by six AN molecules, whereas in the 4/1 phase, they are tetrahedrally coordinated by four AN molecules. The 1/1 solvate further complicates the coordination, leading to an aggregated solvate (AGG) structure. For AN–LiPF₆ mixtures, the 6/1 phase shows Li^+ cations coordinated by four AN molecules, with uncoordinated PF₆[–] anions, while the 5/1 phase differs by one fewer AN molecule per Li^+ , impacting thermal properties.³⁹

Crystallinity gaps often emerge between the 4/1 and 1/1 phases, where mixtures fail to fully crystallize and instead form amorphous solids due to slow nucleation or unfavorable packing. Raman spectroscopy provides additional clarity on these phase behaviors, highlighting distinct TFSI[–] conformations in AN–LiTFSI mixtures and revealing the complexity of solvate structures in AN–LiPF₆ systems. These findings underscore the dynamic nature of solvation and its influence on stability and conductivity, which are pivotal for optimizing performance in all-solid-state batteries (Table 1).

2. Thermodynamic and solvation parameters guiding MOSSE stability

Various parameters, including thermodynamic stability, dielectric constant, polarity, and the Gutmann donor number of the electrolyte materials, can be used to predict high-quality MOSSE.

2.1. Thermodynamic factors influencing the formation of the passivation layer at the electrode–MOSSE interface

The formation of interfacial passivation layers at the anode and cathode surfaces is governed by thermodynamic factors, particularly the energy difference between the Fermi levels of the electrodes and the frontier molecular orbitals, such as the highest occupied molecular orbital (HOMO) and lowest



unoccupied molecular orbital (LUMO) of the electrolyte.^{62–64} When the Fermi level of a positive electrode lies below the HOMO of the electrolyte, there is a thermodynamic driving force for electrolyte oxidation. Conversely, on the negative electrode, if its Fermi level is higher than the LUMO of the electrolyte then there is a driving force for electrolyte reduction.

To control electrolyte decomposition, additives are frequently used. As shown in Fig. 6, additives with a higher HOMO energy than that of the electrolyte solvent are preferentially oxidized at lower potential before other solvents. Similarly, additives with a lower LUMO energy, indicating a higher electron affinity, are reduced earlier on the anode, contributing to the formation of stable passivation layers.

As illustrated in Fig. 7, succinonitrile (SN) compounds exhibit the lowest HOMO among the different additives, salts and carbonates indicating that their oxidation occurs at relatively high potentials. Moreover, cosolvents and salt anions modify the relative HOMO–LUMO energies of the electrolyte components, thereby shifting their oxidation and reduction onset potentials.^{69–71}

Among different lithium salts (in red in Fig. 7), lithium hexafluorophosphate (LiPF₆) is the most widely used in battery electrolytes, but it is prone to decompose in the presence of moisture.⁷² Lithium bis(oxalate)borate (LiBOB) and lithium difluoro(oxalato)borate (LiDFOB) are commonly used as additives due to their beneficial impact on the formation of a stable passivation layer. LiFSI, known for its high oxidative stability,⁶⁸ is particularly well suited for high-voltage battery systems.⁴⁸ Nevertheless, LiFSI and LiTFSI are known to corrode aluminum current collectors, which limits their practical application. Interestingly, increasing the salt concentration in the electrolyte reduces the presence of free solvent molecules that could solvate the dissolved aluminum ions. As a result, corrosion is

halted at the first surface layer of the aluminum foil, thereby preventing deeper degradation of the current collector.^{73,74}

For high voltage electrodes, the electrolyte must have high oxidative stability. The use of low oxidative stability solvents, such as ether oxide, can result in oxidative decomposition of the electrolyte during the charging process.⁷⁵ Furthermore, recent advancements have demonstrated strategies to enhance the oxidative stability of electrolytes. For example, in glyme-based electrolytes, the coordination between glyme molecules and lithium cations lowers the HOMO energy level of the ether oxygen in the glyme molecule, thereby reducing its susceptibility to oxidation. Moreover, the absence of an uncoordinated free solvent in the system further improves the oxidative stability of the electrolyte. As shown in Fig. 8, SN has the lowest HOMO of -9.6 eV with a high dielectric constant of $(\epsilon_r) \approx 55$ which can improve the high voltage stability and be compatible with high voltage cathodes.^{76,77}

2.2. Dielectric constant or relative polarity of MOSSEs

The dielectric constant and relative polarity of a solvent influence how electron density is distributed within the solvent, playing a critical role in determining the strength of ion–ion interactions and the degree of salt dissociation in a solution. The dielectric constant, or relative permittivity, reflects the ability of the solvent to reduce electrostatic forces between charged species. In solvents with a high dielectric constant, the coulombic interactions between ions are significantly weakened, resulting in greater salt dissociation, a higher concentration of free ions, and enhanced ionic conductivity. On the other hand, an electrolyte with a low dielectric constant causes limited electrostatic shielding, resulting in stronger coulombic interactions between oppositely charged ions and reduced ion dissociation.⁸⁰

Potential (V) vs. Li/Li⁺

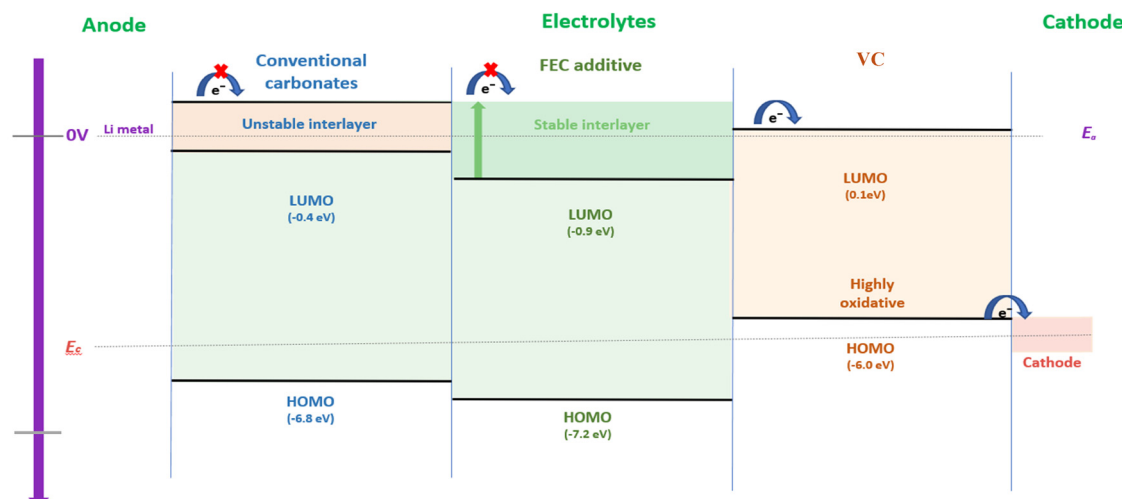


Fig. 6 Schematic illustration of the HOMO–LUMO energy levels of conventional carbonate solvents (e.g., EC/DMC), fluoroethylene carbonate (FEC), and vinylene carbonate (VC) relative to the Li/Li⁺ reference (0 V). VC possesses a higher-lying HOMO than the bulk carbonate solvents, enabling preferential oxidation at high potentials and promoting CEI formation. In contrast, FEC does not have a higher HOMO; its preferential decomposition at the anode arises from its ring-opening reduction chemistry, which facilitates the formation of a stable SEI.^{112–114}



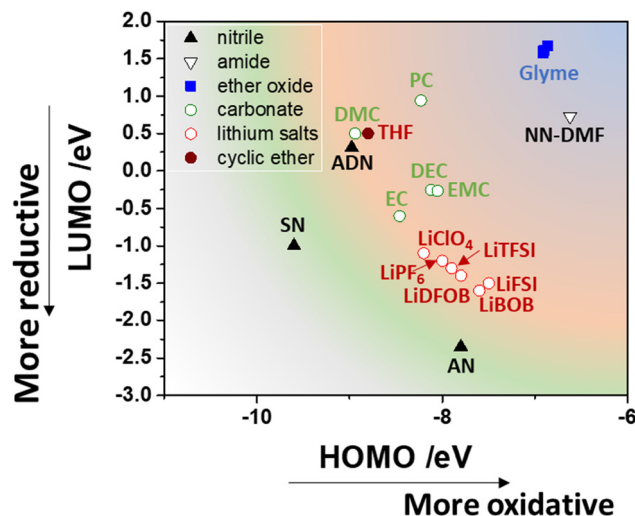


Fig. 7 HOMO and LUMO energies of carbonate, nitrile and glyme-based molecules showing electron donation and acceptance ability.^{65–68}

2.3. Gutmann donor and acceptor numbers

The donor and acceptor numbers, introduced by Gutmann *et al.*, quantify a chemical species ability to donate or accept electron pairs, respectively. Lewis acids are molecules or ions that can accept an electron pair due to the presence of vacant orbitals, resulting in chemical bonding or interactions.^{81–83} Whereas, Lewis bases possess electron pairs that can coordinate with a Lewis acid. In lithium-ion battery systems, the lithium ion functions as a Lewis acid, and the solvents that solvate it act as Lewis bases. As such, the donor number (DN) becomes a crucial parameter influencing electrolyte behaviour.

The DN reflects the strength of interaction between Li^+ and solvent or anion species in the electrolyte. Solvents with low polarity, low dielectric constants, and very low DN values generally have poor lithium salt solubility, making them ineffective as primary solvents. In contrast, many high-polarity

solvents, while capable of dissolving lithium salts, can be overly reactive with lithium metal.⁸⁰ Correlating the Gutman donor number with dielectric constant or polarity of a solvent solubility leads to a useful guiding principle: solvents with low DN that do not dissolve lithium salts act as diluents, whereas those with higher DN values that support salt dissolution function as co-solvents.⁸⁴

Solvents capable of dissolving and dissociating lithium salts at high concentrations tend to have high dielectric constants and high viscosities due to their strong polarity (Fig. 9). The viscosity is inversely proportional to mobility ($\mu = e/6\pi\eta$). Therefore, reducing viscosity is essential for enhancing lithium-ion mobility.⁸⁶ To achieve high ionic conductivity, an ideal electrolyte should combine low viscosity with a high dielectric constant. This is why current organic electrolytes often utilize solvent mixtures: a high-dielectric-constant solvent to effectively dissociate lithium salts, paired with a low-viscosity, low-dielectric-constant solvent to improve mobility. The most common formulation includes a cyclic carbonate such as ethylene carbonate (EC) with a high dielectric constant ($\epsilon_r \approx 90$), mixed with linear carbonates like dimethyl carbonate (DMC), diethyl carbonate (DEC), or ethyl methyl carbonate (EMC), which have much lower dielectric constants ($\epsilon_r \approx 3$) but with viscosities less than 1 cP. Additionally, additives with high donor numbers can strongly coordinate with lithium ions and are used to tailor the morphology of the resulting interphase layer, contributing to improved mechanical flexibility and interfacial stability.^{83,87}

3. MOSSE families

3.1. Glyme-based MOSSEs (ether-oxide)

The study of lithium salt solvates using glymes as molecular solvents can be traced back to the 1990s. Glymes, with the general formula $\text{CH}_3\text{O}-(\text{CH}_2\text{CH}_2\text{O})_n-\text{CH}_3$ (where $n = 1–5$), were extensively compared to polymers in their role as solvents for lithium salts. Notably, Andreev *et al.*⁸⁸ examined the crystal structures of complexes formed between diglyme and lithium salts, specifically $(\text{diglyme})_2\text{LiBF}_4$ and $(\text{diglyme})_2\text{LiSbF}_6$. These complexes exhibit a distorted octahedral geometry around the lithium ion, with each diglyme molecule donating three ether oxygen atoms to coordinate the lithium ion. The structure involves stacking of diglyme complexes, with BF_4^- anions positioned between the layers of diglyme molecules.

The coordination environment varies: in $(\text{diglyme})_2\text{LiBF}_4$, the lithium ion is surrounded by six ether oxygen atoms, while in $(\text{diglyme})\text{LiBF}_4$, the coordination number is reduced to three. This difference in coordination influences the physical properties of the complexes, including ionic conductivity and mechanical strength. A higher coordination number (as in $(\text{diglyme})_2\text{LiBF}_4$ with six ether oxygens around Li^+) leads to a fully solvated cation with minimal Li^-BF_4^- interaction, which tends to increase ionic conductivity.⁸⁹ However, this 2:1 diglyme complex is a discrete molecular unit lacking a polymeric network, so it offers little mechanical strength

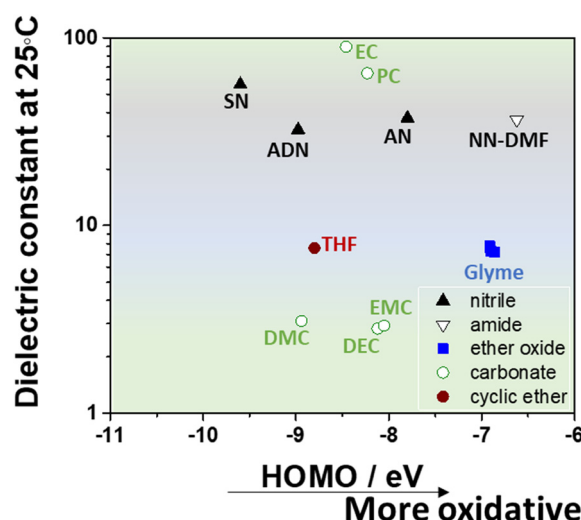


Fig. 8 Dielectric constant vs. HOMO energies for carbonate, nitrile and glyme-based molecules.^{77–79}



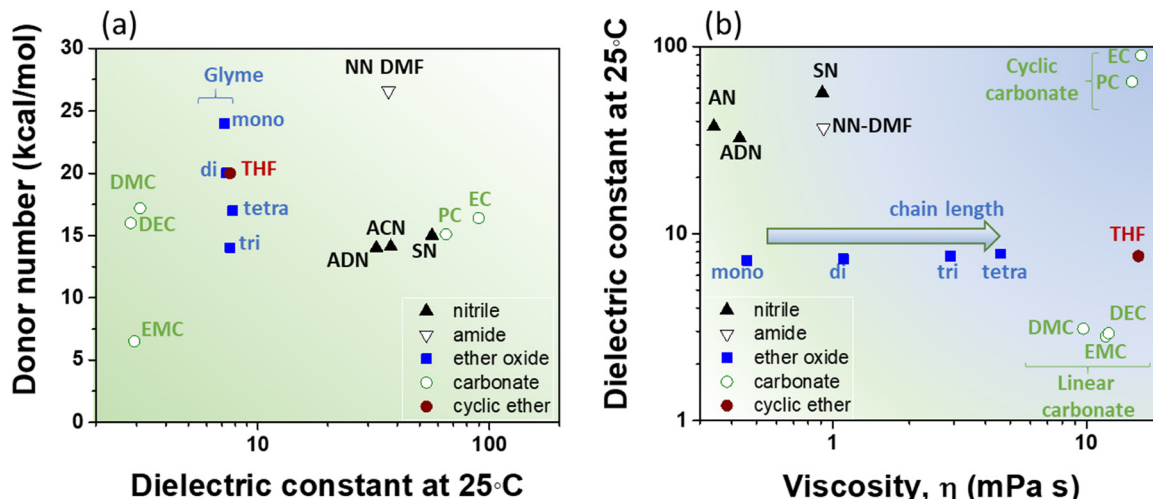


Fig. 9 (a) Gutmann's donor number vs. dielectric constant. (b) Dielectric constant vs. viscosity for carbonate, glyme, and nitrile molecules.⁸⁵

(essentially behaving like a liquid or low-melting solid). In contrast, the 1:1 complex (diglyme : LiBF₄) has Li⁺ coordinated by only three ether oxygens, with BF₄⁻ anions bridging between Li⁺ centers; this stronger Li⁺-anion association reduces ionic mobility (lower conductivity).⁸⁹ The 1:1 complex forms a more rigid crystalline lattice than the 2:1 complex. In contrast to polyethylene oxide (PEO) complexes, which typically adopt a helical structure with isolated polymer chains contributing to both conductivity and mechanical stability, glymes form discrete, coordinated units. This difference in structural organization affects their overall ionic conductivity and mechanical behavior, with glymes offering a distinct coordination pattern compared to polymer-based electrolytes.

Henderson *et al.*^{28,37,38} discussed glyme mixtures with LiTFSI or lithium bis(pentafluoroethylsulfonyl)imide (LiBETI), where Li⁺ cations are typically solvated by ether oxygens as solvent-separated ion pairs (SSIPs). Contact ion pairs (CIPs) and aggregates (AGGs) form when fewer ether oxygens are available. LiTFSI crystal structures show TFSI⁻ anions in transoid form conformation coordinated to four Li⁺ cations, while in monohydrate solvates, TFSI⁻ anions adopt cisoid form conformation. The crystal structures of various LiTFSI and LiBETI solvates exhibit differences in cation coordination and anion conformations, influencing their melting points and phase behaviors.

Phase diagrams for glyme-LiX mixtures indicate various crystalline phases and solid-solid phase transitions, highlighting similarities and differences between TFSI⁻ and BETI⁻ anions in coordination and phase behavior. Raman spectroscopy and DSC analyses further elucidate the phase transitions and structural properties of these solvates, with some forming amorphous phases or showing order-disorder transitions at low temperatures. Notably, increasing ionic association strength leads to decreased crystallinity and the emergence of “crystallinity gaps”, as observed in glyme-LiTFSI and LiBETI mixtures, where amorphous phases persist due to poor structural alignment between solvated ions. This behavior also affects viscosity, with more associated or aggregated phases

typically showing higher viscosities due to stronger ion-solvent interactions and reduced mobility in the disordered matrix.

Seneviratne *et al.*⁹⁰ provided a detailed analysis of the crystal structure and vibrational spectroscopy of diglyme-LiSbF₆ solutions. They discovered and analyzed the structure of the (diglyme)₂LiSbF₆ compound, which crystallizes in the orthorhombic Pccn space group. The unit cell contains four asymmetric units, each comprising a diglyme molecule, half a Li⁺ cation, and half an SbF₆⁻ anion, leading to six-fold coordination of the Li⁺ by two diglyme molecules. The SbF₆⁻ ion shows static disorder, and no direct interaction is found between the cation and the anion. The diglyme molecules adopt a conformation with bonds that are *trans* or *gauche*, similar to the conformation in the (diglyme)LiCF₃SO₃ crystal.

Zhang *et al.*⁴² studied two such complexes, [CH₃O(CH₂CH₂O)₃CH₃] (G3) and [CH₃O(CH₂CH₂O)₄CH₃] (G4), revealing distinct crystal structures and significant differences in their ion transport numbers ($t^+ = 0.8$ for G3 and 0.1 for G4), despite similar conductivities. G3 forms Li⁺ ion-conducting tunnels, unlike G4, where Li⁺ transport pathways are absent. Conductivity measurements *via* AC impedance spectroscopy showed ion hopping in fixed sites and differing activation energies (55 kJ mol⁻¹ for G3, 68 kJ mol⁻¹ for G4). Nevertheless, ionic conductivities are very low for PEO solvates ($\sigma \sim 10^{-7}$ S cm⁻¹) relative to glyme solvates ($\sigma \sim 10^{-6}$ S cm⁻¹). In PEO, Li⁺ is coordinated along a semi-crystalline polymer backbone and its movement requires segmental chain relaxation, which is hindered at room temperature. In contrast, glyme solvates form discrete molecular coordination units that allow Li⁺ to hop between sites without relying on polymer mobility.

Abouimrane *et al.*⁵⁷ explored the properties of (12-Crown-4) and (18-Crown-6) crown ether complexes with LiTFSI at various molar ratios (Fig. 10). DSC scans reveal distinct thermal behaviors, including new peaks indicating transitions to plastic crystal phases and changes in melting points. For instance, the (12-Crown-4)-LiTFSI 1:1 complex shows transition at -109 °C and 88 °C, with melting at 145 °C, while varying ratios



exhibit different thermal behaviors and complex formations. The (18-crown-6)-LiTFSI 1:1 complex exhibits a melting point of 49 °C, which is higher than the ~40 °C melting point of the neat crown ether and an entropy of fusion aligning with Timmerman's criterion. In the plastic phase, these crown-ether-LiTFSI complexes typically reach ionic conductivities on the order of 10^{-5} – 10^{-6} S cm⁻¹ (e.g., $\sim 6 \times 10^{-5}$ S cm⁻¹ at 40 °C for the 18-crown-6 complex), which places them within the range of moderate solid-state ion conductors.⁵⁷

Conductivity measurements indicate significant variance with temperature, with the 1:1 complex showing the highest conductivity in the plastic phase. The (18-crown-6)-LiTFSI 1:1 complex was tested in a lithium-metal battery, demonstrating an electrochemical stability window of at least 4 V and promising but low discharge capacity. These findings reinforce the well-established utility of crown ethers in forming ion-conducting complexes with Li salts, particularly in enabling plastic crystal behavior and moderate conductivity. The thermal and electrochemical insights add to the extensive body of work on crown ether-based electrolytes.

3.2. Succinonitrile-based MOSSEs

Considering that the plastic crystal matrix should act merely as the 'solid solvent' for the dopant ions, providing appropriate mechanical and transport properties, an ideal candidate for novel fast ion conductors would be a molecular plastic crystal capable of dissolving salts. As shown in Fig. 9a, succinonitrile exhibits a plastic phase from –35 °C to 62 °C, featuring a high dielectric constant ($\epsilon = 55$ at 25 °C) and low Gutmann donor number (15), indicating limited cation solvation.⁹¹ Its plasticity suggests suitability as a solid electrolyte in lithium batteries.

Long *et al.*⁴⁵ explored the possibility of creating solid-state electrolytes based on plastic crystalline solvents by doping lithium salts and acids into the plastic crystal phase of succinonitrile. They achieved room temperature conductivities up to 3.4×10^{-4} S cm⁻¹ with 5 wt% LiTFSI in succinonitrile. Pulsed field gradient nuclear magnetic resonance (PFG-NMR) measurements indicated that both cation and anion are mobile in this lattice.

At the same time, Alarco *et al.*²⁴ further investigated the plastic-crystalline phase of succinonitrile as a universal matrix for solid-state ionic conductors. Various salts, including weakly coordinating (TFSI[–]) and strongly coordinating anions (SN[–]), were tested as dopants, producing mechanically stable films with no solubility issues. Conductivity measurements revealed high performance at room temperature and below, with succinonitrile along 5 mol% NH₄TFSI showing 3.16 mS cm⁻¹. The conductivity varied with dopant nature and concentration, generally higher for monovalent cations and lower for divalent and trivalent cations. TFSI salts showed exceptional conductivity due to low lattice energy and high solubility.

Complementing these electrochemical studies, Burba and Powell⁹² provided fundamental structural insights into these systems by isolating a 1:1 solvate of succinonitrile and lithium thiocyanate. Crystallographic analysis identified the structure as a one-dimensional coordination polymer, catena-poly[lithium- μ -thiocyanato-lithium- μ -butanedinitrile], in which lithium ions are

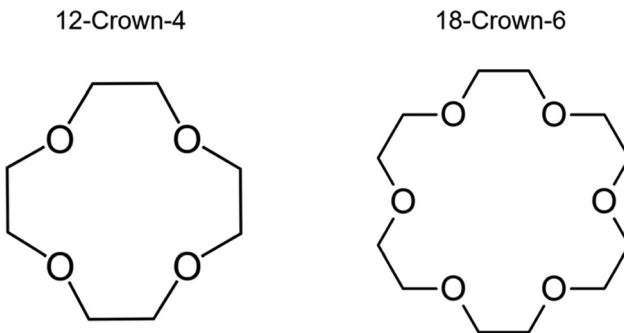


Fig. 10 Schematic structure of 12-crown-4 and 18-crown-6 ethers.

tetrahedrally coordinated by nitrile groups from the solvent and bridging thiocyanate anions. The resulting network consists of double chains linked by Li₂(SN)₂ dimers. Notably, the succinonitrile molecules within this solvate adopt a *gauche* conformation similar to the low-temperature phase of the pure material. These crystallographic findings reveal specific cation-solvent and cation-anion interaction motifs that are essential for guiding the design of next-generation plastic crystalline electrolytes.

Electrochemical tests demonstrated wide voltage windows and high charge-discharge efficiencies for LiFePO₄ and LiCoO₂ cathodes, indicating succinonitrile-based electrolytes' potential for high-performance lithium batteries. The study emphasized the role of anion selection and the plastic-crystal state in enhancing solid electrolyte properties.

Sun *et al.*⁴⁹ utilized a 5 mol% LiTFSI/SN plastic crystal electrolyte (PCE) to address the poor electrochemical performance of organic quinone cathode materials due to their tendency to dissolve in conventional liquid electrolytes. The integration of the SN-based PCE with a calix[4]quinone (C4Q) cathode successfully alleviated this dissolution problem, leading to a high-performance organic lithium-ion battery. This full cell exhibited an initial capacity of 424 mAh g⁻¹ and demonstrated superior cyclic stability, retaining 60% of its initial capacity after 1000 cycles at 0.1C, thus validating the practical application of these MOSSEs in robust, high-energy-density devices.

3.3. Acetonitrile-based MOSSEs

In recent research, it was shown that low concentrations of acetonitrile (AN) (1%) in mixed electrolytes formed stable solid electrolyte interphases (SEIs) on Li metal. As mentioned earlier, the reductive stability of acetonitrile (AN) was improved in concentrated (>4 M) salt solutions, as all of the acetonitrile molecules were coordinated to Li⁺ ions. In dilute solutions, the lowest unoccupied molecular orbital (LUMO) is based on AN molecules, while in super concentrated solutions, the LUMO is localized on the TFSI[–] anion, preventing reductive degradation of the nitrile and suggesting plausibility of anion reduction during charging.⁹³

Seo *et al.*³⁹ explored the solvation behavior and ionic association in acetonitrile-lithium salt mixtures, specifically focusing on highly dissociated salts. They investigated the solid-state

and solution structures of electrolyte mixtures composed of AN with either LiTFSI or LiPF₆ using phase diagrams and Raman spectroscopy. Both salts form a 6/1 AN/LiX crystalline phase, not observed in salts with stronger ion pairing (*i.e.*, less dissociated salts). LiPF₆ creates crystalline phases with high melting points, whereas LiTFSI forms phases that melt at lower temperatures. As a result, (AN)_n–LiTFSI mixtures remain liquid at –30 °C over a broad concentration range, while (AN)_n–LiPF₆ mixtures, except for the most dilute, readily crystallize at ambient temperature.

In dilute mixtures, LiPF₆ and LiTFSI exhibit high levels of dissociation, respectively. When contact ion pairs (CIP) or aggregates (AGG) form, bidentate coordination of Li⁺ cations is more prominent with TFSI[–] anions than with PF₆[–] anions. Quantum chemistry calculations and molecular dynamics simulations further complemented this study. The thermal phase behavior, spectroscopic analysis, and structural information from crystalline solvates and simulations provide valuable insights into the solution structure of these electrolytes.

Yamada *et al.*⁹³ discussed the development of a stable electrolyte for fast-charging, high-voltage lithium-ion batteries using acetonitrile. AN has intrinsically high oxidative stability due to its low-lying HOMO energy level, making it resistant to oxidation even at elevated voltages. However, its reductive stability is typically poor in dilute solutions, where uncoordinated molecules are reduced to cyanide species. In superconcentrated electrolytes (*e.g.*, 4.2 mol dm^{–3} LiTFSI in AN), all AN molecules coordinate with Li⁺, shifting the LUMO from AN to the TFSI[–] anion. This coordination suppresses solvent reduction, stabilizing the electrolyte against lithium metal and enabling reversible lithium plating and graphite intercalation.⁹³

This stability facilitated reversible lithium metal deposition and intercalation into natural graphite electrodes without surface treatments, achieving near-theoretical capacities (330 mAh g^{–1}) and suggesting that TFSI[–] anions, rather than AN solvent, form a protective surface film. Raman spectroscopy and DFT-MD simulations revealed unique solvation structures in superconcentrated solutions, where AN molecules coordinate exclusively with Li⁺ ions, and TFSI[–] anions predominate in the conduction band, explaining the enhanced stability and reversibility observed experimentally. This “salt-concentrating” strategy extends the utility of graphite electrodes to AN-based electrolytes, highlighting their potential for high-performance lithium-ion batteries.

3.4. DMF-based MOSSEs

Chinnam *et al.*^{21,53} demonstrated a promising approach to increasing the conductivity of soft-solid electrolytes by creating crystals with channel walls that have a low affinity for the enclosed ions. Specifically, NN DMF donors, with their soft C=O functionality, interact poorly with hard Li⁺ ions. The co-crystallization of DMF with LiCl results in low-affinity ion channels, enhancing the conductivity properties of the resulting organic solid-state electrolyte.

Single-crystal X-ray diffraction of the 1:1 LiCl·DMF adduct shows the formation of one-dimensional ionically bonded Li₂Cl₂ rhombs interacting with the DMF matrix. This structure facilitates ion migration and results in a room temperature conductivity of 1.6×10^{-4} S cm^{–1}. Remarkably, despite their hygroscopic nature, these DMF·LiCl crystals maintain their integrity in airtight conditions and exhibit stable conductivity. The conductivity decreases at elevated temperatures due to the decomposition of DMF, and Nyquist plots reveal that the conductivity is primarily attributed to bulk resistance rather than grain boundary resistances.

In addition to lithium salts, the research group also explored sodium-based MOSSEs. Specifically, they investigated tris(*N,N*-dimethylformamide)perchloratosodium $[(\text{DMF})_3\text{NaClO}_4]$ cocrystals, which exhibit unique behavior under pressure and temperature changes.⁵⁴ These cocrystals can expel and reabsorb DMF, forming a reversible stoichiometric solvate sponge crystal. This property, along with a low activation energy for Na⁺ ion hopping (25 kJ mol^{–1}), enhances ionic conductivity and presents potential for application in sodium-based solid-state batteries.

Molecular dynamics simulations and experimental techniques were employed to explore the thermomechanical behavior of these cocrystals, offering insights into their structural transformations and ion conduction mechanisms. The simulations showed that sodium ions conduct through a one-dimensional channel and that their conduction is vacancy-driven. The transference number for Na⁺ ions is 0.43 at room temperature and exceeds 0.5 at higher temperatures in the molten mixture. The calculated activation energy for Na⁺ ion diffusion from molecular dynamics simulations is 45 kJ mol^{–1}, and the minimum-energy path of Na⁺ ion migration in the 3:1 crystal provides a barrier of 33 kJ mol^{–1} for Na⁺ ion conduction, in reasonable agreement with experimental values.^{54,55}

These studies underscore the potential of DMF-based MOSSEs as solid electrolytes, especially when considering both lithium and sodium ion conduction. However, challenges such as thermal stability and optimizing the structural arrangement for improved ionic conductivity remain areas for further research.

3.5. Other MOSSE systems

Beyond DMF-based systems a range of other MOSSE architectures have been developed by pairing lithium salts with structurally diverse organic donors. One such example is an isoquinoline-based cocrystal, which offers a markedly different molecular framework and thermal behavior compared to DMF solvates.

To further increase thermal stability and explore materials with potentially better performance, an organic soft base, isoquinoline (IQ), was selected. Isoquinoline, with its aromatic rings, exhibits π -stacking interactions, attractive, non-covalent forces between the delocalized electron clouds of adjacent aromatic rings.⁹⁴ These π – π interactions can enhance intermolecular cohesion, contributing to the structural rigidity and thermal stability of the assembled material. However, in the case of IQ₃·(LiCl)₂, π – π stacking plays a secondary role: the



primary origin of the rigidity arises from the structural arrangement of well-separated Li_4Cl_4 clusters, which are isolated by intervening IQ ligands and lack any continuous pathways for molecular reorientation. This cluster separation and fixed Li-Cl coordination geometry strongly suppress the molecular mobility required for plastic or amorphous phases. In this case, the crystal structure $\text{IQ}_3\cdot(\text{LiCl})_2$ was formed, comprising Li_4Cl_4 (iso-quinoline) molecular units interconnected *via* edge-fused Li_2Cl_2 linkages. Single-crystal X-ray diffraction confirmed the highly crystalline nature of the complex, with a well-ordered three-dimensional framework that reflects its solid-state, non-plastic characteristics. No evidence of amorphous or plastic crystal phases was observed, reinforcing its categorization as a rigid crystalline electrolyte.⁹⁴

Electrochemical impedance spectroscopy revealed that ionic conduction within $\text{IQ}_3\cdot(\text{LiCl})_2$ occurs predominantly through a bulk hopping mechanism, rather than *via* segmental motion or flexible pathways typically seen in polymeric or gel-like systems. The measured activation energy for lithium-ion transport was relatively high (67 kJ mol^{-1}), and the room-temperature conductivity was poor ($\sim 10^{-7} \text{ S cm}^{-1}$), due to the large spatial separation between Li_4Cl_4 clusters imposed by the bulky IQ ligands. This rigid structural arrangement, though beneficial for thermal and structural stability up to $\sim 100^\circ\text{C}$, significantly impedes ion mobility. As a result, the material lacks both the plasticity and ionic conductivity required for high-performance solid-state electrolytes, underscoring the trade-offs associated with crystal engineering strategies that prioritize thermal robustness over ionic transport pathways.⁹⁴

More recently, Fall *et al.*⁴⁷ reported on $(\text{ADN})_2\text{LiPF}_6$, despite the low solubility of LiPF_6 in ADN and the fact that the preparation temperature exceeds the decomposition temperature of LiPF_6 . The complex shows adiponitrile-based channels that facilitate the migration of $-\text{C}\equiv\text{N}-$ solvated Li^+ ions. This material exhibits high ionic conductivity ($\sim 10^{-4} \text{ S cm}^{-1}$) and a high lithium-ion transference number ($t_{\text{Li}^+} = 0.54$). The crystal's surface nanolayer enables the easy formation of ionically conductive pellets. $(\text{ADN})_2\text{LiPF}_6$ widens the electrochemical stability window (0 to 5 V) and demonstrates robust cycling performance in $\text{Li}/(\text{ADN})_2\text{LiPF}_6/\text{LiFePO}_4$ half-cells. Molecular dynamics simulations and density functional theory calculations provided insights into the electrolyte's molecular properties.⁴⁷

Unlike inorganic solid electrolytes, soft-solid crystals like $(\text{ADN})_2\text{LiPF}_6$ enable Li^+ ion migration mediated by organic solvents present at the grain boundaries. Future improvements in conductivity are anticipated through the synthesis of two-dimensional (2D) or three-dimensional (3D) channel systems, optimal solvent and anion engineering, and defect introduction strategies.⁴⁷

Dokko *et al.*⁶⁰ demonstrated that in highly concentrated liquid electrolytes composed of LiBF_4 and sulfolane (SL), Li^+ hopping occurs, deviating from conventional models like Onsager's theory and Stokes' law.⁶⁰ This behavior was confirmed by measuring self-diffusion coefficients using PFG-NMR, revealing faster diffusion of Li^+ compared to SL and BF_4^- at SL/ LiBF_4 molar ratios ≤ 3 .

X-ray crystallographic analysis of the LiBF_4/SL solvate (1:1) and Raman spectra suggest that Li^+ ions are bridged by SL and BF_4^- even in the liquid state, facilitating Li^+ hopping from one coordination site to another. This phenomenon, supported by molecular dynamics simulations, suppresses concentration polarization in lithium batteries, enhancing limiting current density and rate capability. Their findings indicate that Li^+ hopping in concentrated SL electrolytes represents a new understanding of such unconventional systems, with potential implications for improved battery performance.⁶⁰ Franko *et al.* have also reported similar behaviour in the case of ADN and LITFSI as supported also by PFG-NMR and correlations of binary phase diagrams and ionic conductivity isotherms.⁹⁵ This was explained by Abu-Lebdeh's model for electrolyte solutions where the sub-microstructural changes that take place at the eutectic composition switch the transport mechanism from vehicular to hopping.^{29,32,96,97}

In another study, Philippi *et al.*⁹⁸ screened numerous anions for lithium battery electrolytes with high lithium transference numbers using a variety of theoretical and experimental methods. They compared anions based on their stabilization energy, specific interactions with Li^+ , degree of fluorination, flexibility, viscous flow near the glass transition, structural relaxation, ion aggregation, and other properties. They focused on three promising electrolytes: $[\text{Li}(\text{SL})_2][\text{TfNMs}]$, $[\text{Li}(\text{SL})_2][\text{TfNCN}]$, and $[\text{Li}(\text{SL})_2][\text{TfNAc}]$, highlighting $[\text{Li}(\text{SL})_2][\text{TfNCN}]$ for its unique behavior in forming cation-rich clusters due to the interaction between its nitrile group and lithium cations.

The study found that to maximize lithium mobility, the coordination tendencies of the solvent and anion should be matched. Additionally, the authors addressed the significant uncertainties in measuring Onsager coefficients, emphasizing the need for well-defined and verifiable methods. Ultimately, their findings suggest that there is no universally optimal anion-solvent combination; success depends on the careful selection and balance of both components.⁹⁹

These explorations of alternative MOSSE systems demonstrate the potential of organic molecules beyond DMF to serve as effective components in solid electrolytes. By tailoring the molecular structure and interactions within these materials, researchers aim to achieve higher ionic conductivities, improved thermal stability, and better compatibility with battery electrodes, thereby advancing the development of high-performance solid-state batteries.

4. MOSSE beyond lithium-ion chemistry

Okamoto *et al.*⁹⁹ demonstrated that the $[\text{NaFSA}]/[\text{SL}] = 1/1$ electrolyte exhibited superior performance in sodium-ion batteries, particularly when compared to the $[\text{NaFSA}]/[\text{G5}] = 1/1$ electrolyte. In $\text{Na}/\text{Na}_{0.44}\text{MnO}_2$ cells, both electrolytes showed reversible charge-discharge behavior with coulombic efficiencies exceeding 99%. However, the $[\text{NaFSA}]/[\text{SL}] = 1/1$ electrolyte

delivered significantly better rate capability, sustaining higher discharge capacities even at increased current densities.

This improved performance is attributed to the higher Na^+ ion transference number and lower interfacial resistance, which together enhance Na^+ ion migration and reduce overpotential during electrochemical reactions. Furthermore, the $[\text{NaFSA}]/[\text{SL}] = 1/1$ electrolyte effectively suppressed reductive decomposition at the hard carbon electrode, ensuring stable operation for over 90 cycles. These findings underscore the electrolyte's potential to improve both the stability and performance of sodium-ion batteries. The combination of efficient ion migration, reduced overpotential, and enhanced stability positions the $[\text{NaFSA}]/[\text{SL}] = 1/1$ electrolyte as a strong candidate for future advancements in sodium-ion battery technology.

Fall *et al.*²³ investigated a solid electrolyte composed of adiponitrile (ADN) and sodium perchlorate (NaClO_4) in a 3 : 1 molar ratio, producing $(\text{ADN})_3\text{NaClO}_4$. This material exhibits high thermal stability up to 150 °C and is melt-castable with a melting temperature (T_m) of 81 °C. The pressed solid demonstrates a high ionic conductivity of $2.2 \times 10^{-4} \text{ S cm}^{-1}$ at room temperature, with a low activation energy of 22 kJ mol⁻¹. The high conductivity is attributed to low-affinity ion-conduction channels and a nano-liquid layer at the grain boundaries. Scanning electron microscopy and molecular dynamics simulations suggest that this nano-liquid layer facilitates Na^+ ion migration. Density functional theory calculations indicate that ion conduction likely occurs through sodium vacancy defects within a three-dimensional bulk conduction network, rather than along grain boundaries.²³ These observations are not contradictory: the nanoliquid grain-boundary layer improves interparticle contact and lowers macroscopic interfacial resistance, thereby assisting overall pellet-level transport, whereas DFT reveals that the intrinsic ion-migration mechanism is dominated by sodium-vacancy hopping within the three-dimensional crystalline bulk. Thus, the grain boundaries facilitate conduction at the mesoscale, but the bulk lattice remains the primary ion-transport pathway.

A separate investigation by Kang *et al.*⁶¹ focused on potassium anodes and demonstrated significantly lower charge transfer resistance compared to liquid electrolytes, indicating more efficient charge transport. Galvanostatic polarization measurements showed that cells with 1K9D, a crystalline organic electrolyte composed of potassium bis(fluorosulfonyl)imide (KFSI) and dimethyl sulfone (DMS) in a 1 : 9 molar ratio, exhibited reduced polarization and a higher K^+ ion transference number (0.75) compared to liquid electrolyte (LE) cells (0.56).

Testing in $\text{K} \parallel \text{KVPO}_4\text{F}$ cells revealed that 1K9D performed better at lower current densities due to improved charge transfer, its rate performance was slightly lower at higher densities, likely due to slower ion conduction. These findings underscore 1K9D's excellent stability and compatibility with potassium metal anodes, making it a promising material for high-voltage potassium batteries. Enhancing its ionic conductivity and optimizing composition or operating conditions could further improve its performance.⁶¹

5. Limitations of MOSSEs

Despite their advantages, molecular organic solid-state electrolytes (MOSSEs) face several challenges that hinder their practical application in commercial batteries. A primary limitation is thermal stability; while MOSSEs are generally stable at moderate temperatures, they can decompose or lose their crystalline structure at elevated temperatures, leading to decreased ionic conductivity and reduced battery performance.¹² Most reported MOSSEs maintain structural and electrochemical stability only up to roughly 80–150 °C. This is adequate for typical battery operating envelopes (−20 to 55 °C, with safety tolerances up to ~90 °C), but below the >200 °C stability often required of ceramic electrolytes used in extreme environments. This thermal sensitivity raises concerns for applications subjected to extreme temperature conditions.

Another critical issue is their reactivity with highly reactive anode materials like lithium and sodium metals. MOSSEs may exhibit insufficient stability when in direct contact with these metals, potentially leading to dendrite formation or electrolyte degradation, which compromises battery safety and lifespan.⁹⁹ Developing a stable solid electrolyte interphase (SEI) is essential for MOSSE systems; although strategies like increasing salt concentration (as shown in AN-based systems) have shown promise, achieving consistently robust SEI formation across different molecular systems remains a significant hurdle. Similarly, forming a stable cathode–electrolyte interphase (CEI) is critical for high-voltage applications, where operation near or beyond the electrolyte's oxidative limit can trigger decomposition unless a protective CEI is formed. Without it, continuous electrolyte breakdown leads to gas evolution, metal dissolution, and cathode surface degradation, ultimately limiting cycling life and voltage stability. This issue parallels earlier observations with AN-based systems, where poor SEI/CEI formation led to instability unless the electrolyte was sufficiently concentrated to favor anion-derived interphase layers. Thus, both SEI and CEI stabilization are key to unlocking the full electrochemical potential of MOSSEs.^{100–102}

Scalability and manufacturing present additional obstacles. The precise control required in synthesizing MOSSEs to achieve the desired crystalline structures is challenging to replicate on an industrial scale. Integrating MOSSEs into existing battery production processes would likely necessitate substantial modifications, increasing costs and complexity.^{11,12} Furthermore, the high costs associated with high-purity solvents and salts needed for MOSSE synthesis can be prohibitive,¹² making them less economically competitive compared to established electrolyte technologies.

Another practical hurdle for MOSSEs is the manufacturing of thin, uniform electrolyte films suitable for battery assembly. Solid-state cells demand electrolytes on the order of tens of micrometers thick (comparable to ~20 μm polymer separators) to maximize energy density.¹⁰³ However, forming MOSSEs as free-standing films is non-trivial. These electrolytes are often discovered as crystalline salts or solvates that require precise stoichiometry and may contain volatile components, precluding high-temperature processing or vapor-deposition techniques. Unlike polymer



electrolytes that can be easily solvent-cast, pure MOSSE materials lack an inherent polymeric matrix and thus tend to be mechanically fragile or dimensionally unstable in thin film form. For instance, succinonitrile – a plastic-crystalline MOSSE component, can act as a soft plasticizer; at high concentrations the dimensional stability and strength of an electrolyte membrane are compromised. Utilizing porous supports is an emerging solution to the thin-film challenge faced by MOSSEs. Rather than attempting to fabricate freestanding films, which are often brittle and dimensionally unstable, researchers have demonstrated that MOSSEs can be infiltrated into porous scaffolds that provide mechanical reinforcement and processability. In this approach, a microporous membrane or fibrous substrate is typically dipped into or soaked with a liquid or molten MOSSE precursor, which subsequently solidifies within the scaffold's voids. The result is a reinforced composite electrolyte, wherein the structural framework supplies flexibility and dimensional stability, while the infiltrated MOSSE phase forms continuous ion-conducting pathways. For example, one study infused an electrospun PVDF-HFP fiber mat with a succinonitrile-LiTFSI-based MOSSE, achieving a high room-temperature ionic conductivity of approximately 1 mS cm^{-1} without the presence of any free liquid.¹⁰⁴ The fibrous PVDF-HFP matrix preserved the mechanical flexibility of the membrane, while the interconnected SN-LiTFSI domains within the pores ensured rapid lithium-ion transport throughout the structure. Similarly, *in situ* polymerization of a succinonitrile-based MOSSE inside a commercial glass-fiber separator resulted in a composite electrolyte film with a conductivity of around 0.78 mS cm^{-1} at ambient conditions.¹⁰⁵ The glass-fiber scaffold, in this case, provided rigidity and prevented deformation, while the embedded solid MOSSE phase facilitated ionic conduction across the membrane.¹⁰⁵

In another recent example, a lamellar metal-organic framework (MOF) was used as a nanoporous host to confine a LiTFSI-succinonitrile MOSSE.¹⁰⁶ The resulting composite electrolyte, referred to as LSN-MOF, achieved an ionic conductivity of $7.4 \times 10^{-4} \text{ S cm}^{-1}$ at 25°C and remained electrochemically stable against lithium metal. Notably, the MOF's nanoscale channels induced oriented alignment of the succinonitrile molecules, which not only enhanced structural integrity and suppressed electrolyte leakage but also preserved high ionic conductivity by facilitating directional ion transport.¹⁰⁶ Even commercially available polymer battery separators have proven effective as porous hosts for MOSSEs.¹⁰⁷ For instance, a Celgard 2325 trilayer separator, composed of microporous polypropylene and polyethylene, was impregnated with a polymer-succinonitrile-LiTFSI formulation through a simple dip-coating process. Upon drying, the pores were filled with a solid electrolyte phase that maintained high ionic conductivity and offered improved thermal stability, while the inherent tensile strength of the Celgard film provided robust mechanical support for thin-film handling and integration into solid-state cell assemblies.¹⁰⁷

Another significant challenge is achieving good interfacial contact between MOSSE films and electrode surfaces. Solid-state batteries using MOSSEs often suffer from high interfacial resistance at the cathode.¹⁰⁸ The crystalline MOSSE may not conform perfectly to electrode microstructures, leading to

contact gaps or point contacts that impede ionic transfer. Additionally, some MOSSE components can decompose or lose integrity when directly in contact with reactive electrodes at operating potentials. Recent studies emphasize that specialized fabrication steps are needed to form stable interfaces. For example, Watanabe *et al.*¹⁰⁸ found that adding an ultrathin Li_3PO_4 interlayer between a succinonitrile-based MOSSE ($\text{Li}(\text{FSA})(\text{SN})_2$) and a LiCoO_2 cathode dramatically reduced the interface resistance (to $\sim 24 \Omega \text{ cm}^2$, comparable to liquid-electrolyte cells) and suppressed side reactions, enabling stable cycling up to 4.3 V. Such interface engineering, along with applying pressure during cell assembly to ensure intimate contact, is often required to fully leverage MOSSEs in a battery. Incorporating a percentage of MOSSE as a catholyte in the composite cathode has shown remarkable improvements to the cathode-electrolyte interface.¹⁴

Compatibility with existing battery components is also a concern. Incorporating MOSSEs may require the development of new electrode materials or configurations to ensure optimal performance, adding to the time and expense of battery development. Addressing these challenges will require focused research efforts to develop MOSSEs with enhanced thermal and chemical stability, scalable synthesis methods, and cost-effective materials. Innovations in material science and manufacturing processes could enable MOSSEs to transition from laboratory research to practical commercial applications, ultimately contributing to safer and more efficient energy storage systems.

6. Future directions and research opportunities

Advancing MOSSE technology will require targeted research into developing new molecular structures and compositions. Exploring novel combinations of solvents and salts has the potential to enhance the thermal and electrochemical stability of MOSSEs, addressing current performance limitations but this is not the only way forward. Instead of relying on sequential trial-and-error identification of compatible salt-solvent pairs, future MOSSE research can leverage predictive numerical methods to streamline electrolyte design. In particular, analysis frameworks based on Hansen solubility parameters (HSPs) offer a quantitative means to evaluate component compatibility.^{109,110} Hansen's approach breaks a substance's solvation characteristics into dispersion, polar, and hydrogen-bonding contributions, allowing researchers to predict whether a given solvent will effectively dissolve or co-crystallize with a particular salt. This parameter-driven analysis can identify promising solvent-salt combinations computationally, narrowing down candidates prior to laboratory synthesis. Recent work has even extended HSP techniques to ionic liquids using Walden plot data, underscoring the broad utility of such predictive approaches for ion-solvent systems. By incorporating HSP-based compatibility predictions into MOSSE design, the development process can be accelerated – reducing



experimental iterations and focusing efforts on the most viable electrolyte formulations. Overall, shifting towards such data-driven modeling tools could significantly cut down the time and resources needed to discover next-generation MOSSE materials. Researchers are actively investigating ways to tailor solvate structures to optimize ion transport properties and minimize reactivity with battery components.^{109,110} A key focus area is improving the ionic conductivity of MOSSEs. This may involve designing electrolytes with 2D or 3D ion-conducting channels, optimizing solvent and anion combinations, or introducing defects into the crystal lattice to facilitate ion migration.^{23,47} Enhancing ionic conductivity is crucial for achieving higher battery performance and efficiency. Improving the interfacial properties between MOSSEs and electrode materials is another important aspect. Strategies such as designing additives that form stable, conductive interphases or creating protective coatings to prevent electrode degradation can increase MOSSE versatility and efficiency, making them more applicable across a broader range of battery systems.^{60,98} These approaches aim to reduce interfacial resistance and enhance compatibility with various electrode materials.

Addressing scalability and economic feasibility is also critical. Developing cost-effective synthesis methods and utilizing more readily available materials could make MOSSEs more viable for commercial applications.¹² Efforts to simplify production processes and reduce material costs are essential to facilitate large-scale manufacturing and adoption.¹¹¹

Expanding the application of MOSSEs to beyond-lithium systems presents additional opportunities. MOSSEs hold considerable promise for significantly improving the performance and safety of all-solid-state batteries (ASSBs). Their ability to provide a stable, high-conductivity electrolyte could enable the use of high-energy-density anode and cathode materials, resulting in batteries with greater capacity and longer cycle life.²⁰ Additionally, MOSSEs offer enhanced safety features, such as improved thermal stability and reduced risk of dendrite formation, aligning well with the demands of next-generation battery technologies.

Integrating MOSSEs into ASSBs could lead to more robust and reliable energy storage systems, fostering advancements in electric vehicles, portable electronics, and renewable energy storage solutions. Continued research and development in this area could drive innovation across multiple industries, ultimately leading to more sustainable, high-performance battery technologies.

7. Conclusions

The exploration of molecular organic solid-state electrolytes (MOSSEs) reveals a versatile and under-recognized class of materials capable of addressing long-standing limitations in solid-state ion transport. By leveraging weakly coordinating organic molecules to build soft-crystalline, ion-conducting frameworks, MOSSEs occupy a unique middle ground between rigid inorganic ceramics and low-conductivity polymers. Their

structural diversity spanning glyme solvates, succinonitrile plastic crystals, adiponitrile-based systems, superconcentrated acetonitrile cocrystals, and related donor–salt architectures—demonstrates that organic molecular design can yield solid electrolytes with competitive conductivities (often 10^{-4} – 10^{-3} S cm $^{-1}$), melt-processability, and mechanically compliant lattices that can adapt to electrode interfaces.

Among the MOSSE systems surveyed, several families emerge as particularly promising depending on the targeted performance metric. Glyme-based solvates remain among the most mature, offering well-defined stoichiometries, persistent cation–solvent coordination motifs, and oxidative stability extending to \sim 5 V, with ionic conductivities in the 10^{-4} – 10^{-3} S cm $^{-1}$ range. Succinonitrile-based plastic crystals stand out for their exceptional mechanical compliance, high dielectric screening, and melt-castability, which together facilitate low interfacial resistance and robust ion transport. Adiponitrile-based crystalline systems provide a compelling balance of conductivity, broad electrochemical stability windows, and demonstrated Na^+/Li^+ transport in practical cells aided by nano-liquid grain-boundary layers. Superconcentrated acetonitrile-based MOSSEs further distinguish themselves by achieving remarkable anodic stability and compatibility with lithium metal through anion-derived interphases.

Importantly, solvate-based MOSSEs form a structurally distinct subset whose microstructure is fundamentally dictated by phase-diagram positioning. At the precise solvate composition, the salt and solvent co-crystallize into stoichiometric, single-phase lattices where solvent molecules become integral components of the crystal architecture. This generates uniform coordination environments, well-aligned ion-transport channels, and intrinsic or thermally activated vacancy-mediated pathways. These ordered microstructures explain the high thermal stability, reproducible transport behavior, and melt-castability observed in systems such as LiTFSI-3DME, (G2) $_2$:LiTFSI, and AN $_6$:LiX phases. Off-stoichiometric compositions, in contrast, frequently yield biphasic or metastable solids with reduced and less predictable electrochemical performance. Systematic exploration of solvate ratios across full salt–solvent phase diagrams therefore represents a particularly powerful route for discovering next-generation MOSSEs. The solvate points, not arbitrary mixtures, mark the compositions where the most stable crystal structures, most efficient transport pathways, and most favorable interfacial behaviors emerge. Expanding this library across donor families and anion chemistries could unlock MOSSE candidates with tailored conductivity, enhanced stability, and improved processability.

Despite their promise, several challenges remain, most notably thermal stability limits for certain donor molecules, mechanical fragility in thin-film geometries, and chemical reactivity at high-voltage or lithium–metal interfaces. Nonetheless, recent progress in interphase engineering, composite scaffolding, and melt-casting strategies highlights practical pathways toward addressing these barriers. Collectively, the soft-crystalline nature, tunable structural motifs, and favorable transport characteristics of MOSSEs position them as strong



contenders for enabling safer, more efficient, and higher-energy solid-state batteries. Continued interdisciplinary research, bridging molecular design, electrochemistry, and device engineering, will be essential to realizing the full technological potential of this emerging electrolyte family.

Conflicts of interest

There are no conflicts to declare.

Data availability

No primary research results, software or code have been included and no new data were generated or analysed as part of this review.

Acknowledgements

We would like to thank Mr Xue Lin Chin for his valuable efforts in compiling the data for this work. We also thank the Canada Critical Battery Materials Initiative (CBMI) for funding this research.

References

- 1 K. Xu, Electrolytes and interphases in Li-ion batteries and beyond, *Chem. Rev.*, 2014, **114**, 11503–11618.
- 2 S. Raza, *et al.*, Recent progress and fundamentals of solid-state electrolytes for all solid-state rechargeable batteries: Mechanisms, challenges, and applications, *J. Energy Storage*, 2024, **92**, 112110.
- 3 H. Al-Salih, E. Baranova and Y. Abu-Lebdeh, Solid-state batteries: The interfacial challenge to replace liquid electrolytes. *Encyclopedia of Solid-Liquid Interfaces*, 2024, pp. 444–453, DOI: [10.1016/B978-0-323-85669-0.00146-X](https://doi.org/10.1016/B978-0-323-85669-0.00146-X).
- 4 J. M. Tarascon and M. Armand, Issues and challenges facing rechargeable lithium batteries, *Nature*, 2001, **414**, 359–367.
- 5 H. Al-Salih, H. A. Khan, E. A. Baranova and Y. Abu-Lebdeh, Back to the future: towards the realization of lithium metal batteries using liquid and solid electrolytes, *Front. Energy Res.*, 2023, **11**, 1325316.
- 6 D. Lin, Y. Liu and Y. Cui, Reviving the lithium metal anode for high-energy batteries, *Nat. Nanotechnol.*, 2017, **12**, 194–206.
- 7 X. B. Cheng, R. Zhang, C. Z. Zhao and Q. Zhang, Toward Safe Lithium Metal Anode in Rechargeable Batteries: A Review, *Chem. Rev.*, 2017, **117**, 10403–10473.
- 8 V. Thangadurai, S. Narayanan and D. Pinzaru, Garnet-type solid-state fast Li ion conductors for Li batteries: Critical review, *Chem. Soc. Rev.*, 2014, **43**, 4714–4727.
- 9 X. Li, *et al.*, Progress and perspectives on halide lithium conductors for all-solid-state lithium batteries, *Energy Environ. Sci.*, 2020, **13**, 1429–1461.
- 10 Z. Karkar, *et al.*, An Industrial Perspective and Intellectual Property Landscape on Solid-State Battery Technology with a Focus on Solid-State Electrolyte Chemistries, *Batteries*, 2024, **10**(1), 24.
- 11 A. Banerjee, X. Wang, C. Fang, E. A. Wu and Y. S. Meng, Interfaces and Interphases in All-Solid-State Batteries with Inorganic Solid Electrolytes, *Chem. Rev.*, 2020, **120**, 6878–6933.
- 12 Q. Zhao, S. Stalin, C.-Z. Zhao and L. A. Archer, Designing solid-state electrolytes for safe, energy-dense batteries, *Nat. Rev. Mater.*, 2020, 1–24, DOI: [10.1038/s41578-019-0165-5](https://doi.org/10.1038/s41578-019-0165-5).
- 13 H. Al-Salih, *et al.*, A Polymer-Rich Quaternary Composite Solid Electrolyte for Lithium Batteries, *J. Electrochem. Soc.*, 2020, **167**, 070557.
- 14 H. Al-Salih, M. Seif, E. Houache, E. A. Baranova and Y. Abu-Lebdeh, Composite Cathodes for Solid-State Lithium Batteries: “Catholytes” the Underrated Giants, *Adv. Energy Sustainable Res.*, 2022, **3**, 2200032.
- 15 S. Yan, *et al.*, Engineered Interfaces between Perovskite La₂/3xLi₃Ti₃O₁₂ Electrolyte and Li Metal for Solid-State Batteries, *Front. Chem.*, 2022, **10**, 966274.
- 16 H. Al-Salih, *et al.*, A Ceramic Rich Quaternary Composite Solid-State Electrolyte for Solid-State Lithium Metal Batteries, *J. Electrochem. Soc.*, 2022, **169**, 080510.
- 17 F. Han, *et al.*, Interphase Engineering Enabled All-Ceramic Lithium Battery, *Joule*, 2018, **2**, 497–508.
- 18 Y. Li, *et al.*, Hybrid Polymer/Garnet Electrolyte with a Small Interfacial Resistance for Lithium-Ion Batteries, *Angew. Chem., Int. Ed.*, 2017, **56**, 753–756.
- 19 E. Quartarone, P. Mustarelli and A. Magistris, PEO-based composite polymer electrolytes, *Solid State Ionics*, 1998, **110**, 1–14.
- 20 T. Famprikis, P. Canepa, J. A. Dawson, M. S. Islam and C. Masquelier, Fundamentals of inorganic solid-state electrolytes for batteries, *Nat. Mater.*, 2019, **18**, 1278–1291.
- 21 P. R. Chinnam, R. N. Clymer, A. A. Jalil, S. L. Wunder and M. J. Zdilla, Bulk-Phase Ion Conduction in Cocrystalline LiCl·N,N-Dimethylformamide: A New Paradigm for Solid Electrolytes Based upon the Pearson Hard-Soft Acid-Base Concept, *Chem. Mater.*, 2015, **27**, 5479–5482.
- 22 J. Fraxedas *Molecular Organic Materials: From Molecules to Crystalline Solids - Jordi Fraxedas* - Google Books, Cambridge University Press, 2006.
- 23 B. Fall, *et al.*, Experimental and Theoretical Investigation of the Ion Conduction Mechanism of Tris(adiponitrile)perchloratosodium, a Self-Binding, Melt-Castable Crystalline Sodium Electrolyte, *Chem. Mater.*, 2019, **31**(21), 8850–8863.
- 24 P. J. Alarco, Y. Abu-Lebdeh, A. Abouimrane and M. Armand, The plastic-crystalline phase of succinonitrile as a universal matrix for solid-state ionic conductors, *Nat. Mater.*, 2004, **3**, 476–481.
- 25 R. G. Pearson, Hard and Soft Acids and Bases, *J. Am. Chem. Soc.*, 1963, **85**, 3533–3539.
- 26 S. A. Kirillov, M. I. Gorobets, D. O. Tretyakov, M. B. Ataev and M. M. Gafurov, Phase diagrams and conductivity of lithium salt systems in dimethyl sulfoxide, propylene carbonate and dimethyl carbonate, *J. Mol. Liq.*, 2015, **205**, 78–84.
- 27 S. A. Kirillov, M. I. Gorobets, D. O. Tretyakov, M. B. Ataev and M. M. Gafurov, Phase diagrams and conductivity of lithium salt systems in dimethyl sulfoxide, propylene carbonate and dimethyl carbonate, *J. Mol. Liq.*, 2015, **205**, 78–84.
- 28 W. A. Henderson, Glyme-lithium salt phase behavior, *J. Phys. Chem. B*, 2006, **110**, 13177–13183.
- 29 H. Al-Salih and Y. Abu-Lebdeh, Investigating the phase diagram-ionic conductivity isotherm relationship in aqueous solutions of common acids: hydrochloric, nitric, sulfuric and phosphoric acid, *Sci. Rep.*, 2024, **14**(1), 7894.
- 30 H. Al-Salih and Y. Abu-Lebdeh, Investigating the phase diagram-ionic conductivity isotherms relationship in aqueous solutions of strong bases: Lithium, sodium and potassium hydroxides, *J. Mol. Liq.*, 2025, **422**, 127179.
- 31 E. O. Nachaki and D. G. Kuroda, Lithium ion Speciation in Cyclic Solvents: Impact of Anion Charge Delocalization and Solvent Polarizability, *J. Phys. Chem. B*, 2024, **128**, 3408–3415.
- 32 H. Al-Salih, E. A. Baranova and Y. Abu-Lebdeh, Unraveling the phase diagram-ion transport relationship in aqueous electrolyte solutions and correlating conductivity with concentration and temperature by semi-empirical modeling, *Commun. Chem.*, 2023, **6**, 1–13.
- 33 L. Faro, *et al.*, Importance of High-Concentration Electrolytes for Lithium-Based Batteries, *Encyclopedia*, 2025, vol. 5, p. 20.
- 34 C. Kang, *et al.*, Concentration Induced Modulation of Solvation Structure for High Performance Lithium Metal Battery by Regulating Energy Level of Lumo Orbital. (2023), DOI: [10.2139/SSRN.4348195](https://doi.org/10.2139/SSRN.4348195).
- 35 C. J. Franko, *et al.*, Concentration Dependent Solution Structure and Transport Mechanism in High Voltage LiTFSI-Adiponitrile Electrolytes, *J. Electrochem. Soc.*, 2020, **167**, 160532.
- 36 W. Wang, *et al.*, Stable Cycling of High-Voltage Lithium-Metal Batteries Enabled by High-Concentration FEC-Based Electrolyte, *ACS Appl. Mater. Interfaces*, 2020, **12**, 22901–22909.
- 37 W. A. Henderson, *et al.*, Glyme-lithium bis(trifluoromethanesulfonyl)imide and glyme-lithium bis(perfluoroethanesulfonyl)imide phase behavior and solvate structures, *Chem. Mater.*, 2005, **17**, 2284–2289.

38 W. A. Henderson, N. R. Brooks, W. W. Brennessel and V. G. Young, LiClO₄ electrolyte solvate structures, *J. Phys. Chem. A*, 2004, **108**, 225–229.

39 D. M. Seo, O. Borodin, S.-D. Han, P. D. Boyle and W. A. Henderson, Electrolyte Solvation and Ionic Association II. Acetonitrile-Lithium Salt Mixtures: Highly Dissociated Salts, *J. Electrochem. Soc.*, 2012, **159**, A1489–A1500.

40 D. Brouillette, *et al.*, Stable solvates in solution of lithium bis(trifluoromethylsulfone)imide in glymes and other aprotic solvents: Phase diagrams, crystallography and Raman spectroscopy, *Phys. Chem. Chem. Phys.*, 2002, **4**, 6063–6071.

41 W. A. Henderson, N. R. Brooks, W. W. Brennessel and V. G. Young, Triglyme-Li⁺ Cation Solvate Structures: Models for Amorphous Concentrated Liquid and Polymer Electrolytes (I), *Chem. Mater.*, 2003, **15**, 4679–4684.

42 C. Zhang, D. Ainsworth, Y. G. Andreev and P. G. Bruce, Ionic conductivity in the solid glyme complexes [CH₃O(CH₂CH₂O)_nCH₃]:LiAsF₆ (n = 3,4), *J. Am. Chem. Soc.*, 2007, **129**, 8700–8701.

43 K. Yoshida, *et al.*, Oxidative-stability enhancement and charge transport mechanism in glyme-lithium salt equimolar complexes, *J. Am. Chem. Soc.*, 2011, **133**, 13121–13129.

44 M. Watanabe, *et al.*, From Ionic Liquids to Solvate Ionic Liquids: Challenges and Opportunities for Next Generation Battery Electrolytes, *Bull. Chem. Soc. Jpn.*, 2018, **91**, 1660–1682.

45 S. Long, D. R. MacFarlane and M. Forsyth, Fast ion conduction in molecular plastic crystals, *Solid State Ionics*, 2003, **161**, 105–112.

46 A. Abouimrane, P. S. Whitfield, S. Niketic and I. J. Davidson, Investigation of Li salt doped succinonitrile as potential solid electrolytes for lithium batteries, *J. Power Sources*, 2007, **174**, 883–888.

47 B. Fall, A soft co-crystalline solid electrolyte for lithium-ion batteries, *Nat. Mater.*, 2022, **22**, 627–635.

48 Y. Yamada, *et al.*, Unusual stability of acetonitrile-based super-concentrated electrolytes for fast-charging lithium-ion batteries, *J. Am. Chem. Soc.*, 2014, **136**, 5039–5046.

49 H. Sun, *et al.*, High-Performance organic lithium–ion battery with plastic crystal electrolyte, *Org. Electron.*, 2020, **87**, 105966.

50 C. C. Yang, H. Y. Hsu and C. R. Hsu, Transport properties of LiTFSI-acetamide room temperature molten salt electrolytes applied in an Li-Ion battery, *Z. Phys. Chem.*, 2007, **62**, 639–646.

51 M. Moriya, D. Kato, Y. Hayakawa, W. Sakamoto and T. Yogo, Crystal structure and solid state ionic conductivity of molecular crystal composed of lithium bis(trifluoromethanesulfonyl)amide and 1,2-dimethoxybenzene in a 1:1 molar ratio, *Solid State Ionics*, 2016, **285**, 29–32.

52 P. Prakash, *et al.*, Unravelling the structural and dynamical complexity of the equilibrium liquid grain-binding layer in highly conductive organic crystalline electrolytes, *J. Mater. Chem. A*, 2018, **6**, 4394–4404.

53 P. R. Chinnam, *et al.*, A Self-Binding, Melt-Castable, Crystalline Organic Electrolyte for Sodium Ion Conduction, *Angew. Chem., Int. Ed.*, 2016, **55**, 15254–15257.

54 P. Prakash, *et al.*, Solvate sponge crystals of (DMF) 3 NaClO 4: reversible pressure/temperature controlled juicing in a melt/press-castable sodium-ion conductor, *Chem. Sci.*, 2021, **12**, 5574–5581.

55 P. Prakash, *et al.*, Mechanism of Ion Conduction and Dynamics in Tris(N, N-dimethylformamide) Perchloratosodium Solid Electrolytes, *J. Phys. Chem. C*, 2022, **126**, 4744–4750.

56 B. Fall, *et al.*, Crystal structure and ionic conductivity of the soft solid crystal: isoquinoline3 (LiCl)₂, *Ionics*, 2018, **24**, 343–349.

57 A. Abouimrane, P. J. Alarco, Y. Abu-Lebdeh, I. Davidson and M. Armand, Plastic crystalline phases of crown ether:salt complexes and their utilization in lithium-metal batteries, *J. Power Sources*, 2007, **174**, 1193–1196.

58 M. Moriya, D. Kato, W. Sakamoto and T. Yogo, Structural Design of Ionic Conduction Paths in Molecular Crystals for Selective and Enhanced Lithium Ion Conduction, *Chem. – Eur. J.*, 2013, **19**, 13554–13560.

59 D. M. Seo, *et al.*, Structural Interactions within Lithium Salt Solvates: Cyclic Carbonates and Esters, *J. Phys. Chem. C*, 2014, **118**, 25884–25889.

60 K. Dokko, *et al.*, Direct Evidence for Li Ion Hopping Conduction in Highly Concentrated Sulfolane-Based Liquid Electrolytes, *J. Phys. Chem. B*, 2018, **122**, 10736–10745.

61 S. Kang, B. Jeon, S. T. Hong and H. Lee, A sulfone-based crystalline organic electrolyte for 5 V solid-state potassium batteries, *Chem. Eng. J.*, 2022, **443**, 136403.

62 O. Borodin, J. Self, K. A. Persson, C. Wang and K. Xu, Uncharted Waters: Super-Concentrated Electrolytes, *Joule*, 2020, **4**, 69–100.

63 J. B. Goodenough, How we made the Li-ion rechargeable battery: Progress in portable and ubiquitous electronics would not be possible without rechargeable batteries. John B. Goodenough recounts the history of the lithium-ion rechargeable battery, *Nat. Electron.*, 2018, **1**, 204.

64 J. B. Goodenough and Y. Kim, Challenges for rechargeable Li batteries, *Chem. Mater.*, 2010, **22**, 587–603.

65 M. Gauthier, *et al.*, Electrode–Electrolyte Interface in Li-Ion Batteries: Current Understanding and New Insights, *J. Phys. Chem. Lett.*, 2015, **6**, 4653–4672.

66 D. Zhao and S. Li, Regulating the Performance of Lithium-Ion Battery Focus on the Electrode–Electrolyte Interface, *Front. Chem.*, 2020, **8**, 535418.

67 K. Xu, Nonaqueous liquid electrolytes for lithium-based rechargeable batteries, *Chem. Rev.*, 2004, **104**, 4303–4417.

68 S. S. Zhang, A review on electrolyte additives for lithium-ion batteries, *J. Power Sources*, 2006, **162**, 1379–1394.

69 H. Zhi, L. Xing, X. Zheng, K. Xu and W. Li, Understanding How Nitriles Stabilize Electrolyte/Electrode Interface at High Voltage, *J. Phys. Chem. Lett.*, 2017, **8**, 6048–6052.

70 R. Chen, *et al.*, An investigation of functionalized electrolyte using succinonitrile additive for high voltage lithium-ion batteries, *J. Power Sources*, 2016, **306**, 70–77.

71 S. Han, *et al.*, Succinonitrile as a high-voltage additive in the electrolyte of LiNi_{0.5}Co_{0.2}Mn_{0.3}O₂/graphite full batteries, *Surf. Interface Anal.*, 2020, **52**, 364–373.

72 K. Xu, Nonaqueous liquid electrolytes for lithium-based rechargeable batteries, *Chem. Rev.*, 2004, **104**, 4303–4417.

73 Y. Yamada, *et al.*, Corrosion Prevention Mechanism of Aluminum Metal in Superconcentrated Electrolytes, *ChemElectroChem*, 2015, **2**, 1687–1694.

74 C. Zhang, *et al.*, Chelate effects in glyme/lithium Bis(trifluoromethanesulfonyl)amide solvate ionic liquids, Part 2: Importance of solvate-structure stability for electrolytes of lithium batteries, *J. Phys. Chem. C*, 2014, **118**, 17362–17373.

75 M. Gauthier, *et al.*, Probing Surface Chemistry Changes Using LiCoO₂ -only Electrodes in Li-Ion Batteries, *J. Electrochem. Soc.*, 2018, **165**, A1377–A1387.

76 J. Sun, *et al.*, Hierarchical Composite-Solid-Electrolyte with High Electrochemical Stability and Interfacial Regulation for Boosting Ultra-Stable Lithium Batteries, *Adv. Funct. Mater.*, 2021, **31**, 2006381.

77 D. Zhang, *et al.*, Eutectic-Based Polymer Electrolyte with the Enhanced Lithium Salt Dissociation for High-Performance Lithium Metal Batteries, *Angew. Chem.*, 2023, **135**, e202310006.

78 J. Sun, *et al.*, Hierarchical Composite-Solid-Electrolyte with High Electrochemical Stability and Interfacial Regulation for Boosting Ultra-Stable Lithium Batteries, *Adv. Funct. Mater.*, 2021, **31**, 2006381.

79 R. Tatara, Concentrated Electrolytes and Their Unique Interfacial Reactions in Rechargeable Batteries, *Electrochemistry*, 2024, **92**, 101005.

80 R. Tatara, Concentrated Electrolytes and Their Unique Interfacial Reactions in Rechargeable Batteries, *Electrochemistry*, 2024, **92**, 101005.

81 Q. Lin, *et al.*, Perspective on Lewis Acid-Base Interactions in Emerging Batteries, *Adv. Mater.*, 2024, **36**, 2406151.

82 J. F. Gal, P. C. Maria, M. Yáñez and O. Mó, Lewis basicity of alkyl carbonates and other esters. The Gutmann Donor Number (DN), a flawed indicator? Boron trifluoride adduct-formation enthalpy, experimentally or computationally determined, as a reliable alternative, *J. Mol. Liq.*, 2023, **370**, 120997.

83 P. Zhou, Y. Xiang and K. Liu, Understanding and applying the donor number of electrolytes in lithium metal batteries, *Energy Environ. Sci.*, 2024, **17**, 8057–8077.

84 J. Chen, H. Zhang, C. Ke, S. Liu and J. Wang Design localized high concentration electrolytes via donor number and solubility. (2022), DOI: [10.26434/CHEMRXIV-2022-48S6J](https://doi.org/10.26434/CHEMRXIV-2022-48S6J).



85 B. Sanchez, P. R. Campodónico and R. Contreras, Gutmann's Donor and Acceptor Numbers for Ionic Liquids and Deep Eutectic Solvents, *Front. Chem.*, 2022, **10**, 861379.

86 S. S. Sekhon, N. Arora and H. P. Singh, Effect of donor number of solvent on the conductivity behaviour of nonaqueous proton-conducting polymer gel electrolytes, *Solid State Ionics*, 2003, **160**, 301–307.

87 Z. Arain, *et al.*, Elucidating the dynamics of solvent engineering for perovskite solar cells, *Sci. China Mater.*, 2019, **62**, 161–172.

88 Y. G. Andreev, *et al.*, Crystal structures of poly(ethylene oxide):LiBF₄ and (diglyme)_n:LiBF₄ (n = 1,2), *Chem. Mater.*, 2005, **17**, 767–772.

89 Y. G. Andreev, *et al.*, Crystal structures of poly(ethylene oxide):LiBF₄ and (diglyme)_n:LiBF₄ (n = 1,2), *Chem. Mater.*, 2005, **17**, 767–772.

90 V. Seneviratne, R. Frech, J. E. Furneaux and M. Khan, Characterization of Crystalline and Solution Phases of Diglyme–LiSbF₆, *J. Phys. Chem. B*, 2004, **108**, 8124–8128.

91 D. Linden, *Handbook of batteries*, (Fuel and energy abstracts), vol. 4. No. 36, 1995.

92 C. M. Burba, D. R. Powell and M. Zeller, A 1:1 solvate structure of succinonitrile and lithium thiocyanate, *Acta Crystallogr., Sect. E: Crystallogr. Commun.*, 2022, **78**, 1284–1287.

93 Y. Yamada, *et al.*, Unusual stability of acetonitrile-based super-concentrated electrolytes for fast-charging lithium-ion batteries, *J. Am. Chem. Soc.*, 2014, **136**, 5039–5046.

94 B. Fall, *et al.*, Crystal structure and ionic conductivity of the soft solid crystal: isoquinoline3-(LiCl)₂, *Ionics*, 2018, **24**, 343–349.

95 C. J. Franko, *et al.*, Concentration Dependent Solution Structure and Transport Mechanism in High Voltage LiTFSI-Adiponitrile Electrolytes, *J. Electrochem. Soc.*, 2020, **167**, 160532.

96 C.-H. Yim, J. Tam, H. Soboleski and Y. Abu-Lebdeh, On the Correlation between Free Volume, Phase Diagram and Ionic Conductivity of Aqueous and Non-Aqueous Lithium Battery Electrolyte Solutions over a Wide Concentration Range, *J. Electrochem. Soc.*, 2017, **164**, A1002–A1011.

97 C.-H. Yim and Y. A. Abu-Lebdeh, Connection between Phase Diagram, Structure and Ion Transport in Liquid, Aqueous Electrolyte Solutions of Lithium Chloride, *J. Electrochem. Soc.*, 2018, **165**, A547–A556.

98 F. Philippi, *et al.*, Evolving better solvate electrolytes for lithium secondary batteries, *Chem. Sci.*, 2024, **15**, 7342–7358.

99 Y. Okamoto, *et al.*, High Transference Number of Na Ion in Liquid-State Sulfolane Solvates of Sodium Bis(fluorosulfonyl)amide, *J. Phys. Chem. C*, 2020, **124**, 4459–4469.

100 Z. Zhu, *et al.*, Demystifying the Salt-Induced Li Loss: A Universal Procedure for the Electrolyte Design of Lithium-Metal Batteries, *Nano-Micro Lett.*, 2023, **15**, 1–10.

101 M. Li, *et al.*, Acetonitrile-Based Local High-Concentration Electrolytes for Advanced Lithium Metal Batteries, *Adv. Mater.*, 2024, **36**, 2404271.

102 J. Xu, Critical Review on cathode–electrolyte Interphase Toward High-Voltage Cathodes for Li-Ion Batteries, *Nano-Micro Lett.*, 2022, **14**, 1–22.

103 M. Balaish, *et al.*, Processing thin but robust electrolytes for solid-state batteries, *Nat. Energy*, 2021, **63**(6), 227–239.

104 G. Qiu, Y. Shi and B. Huang, A highly ionic conductive succinonitrile-based composite solid electrolyte for lithium metal batteries, *Nano Res.*, 2022, **15**, 5153–5160.

105 Y. Okamoto, *et al.*, High Transference Number of Na Ion in Liquid-State Sulfolane Solvates of Sodium Bis(fluorosulfonyl)amide, *J. Phys. Chem. C*, 2020, **124**, 4459–4469.

106 T. Zhao, *et al.*, Laminar composite solid electrolyte with succinonitrile-penetrating metal-organic framework (MOF) for stable anode interface in solid-state lithium metal battery, *J. Power Sources*, 2023, **554**, 232349.

107 C. Li, *et al.*, A novel composite solid polymer electrolyte based on copolymer P(LA-*co*-TMC) for all-solid-state lithium ionic batteries, *Solid State Ionics*, 2018, **321**, 8–14.

108 Y. Watanabe, *et al.*, Reduced resistance at molecular-crystal electrolyte and LiCoO₂ interfaces for high-performance solid-state lithium batteries, *APL Mater.*, 2025, **13**, 11122.

109 D. M. Koenhen, & Smolders, C. A. The determination of solubility parameters of solvents and polymers by means of correlations with other physical quantities, *J. Appl. Polym. Sci.*, 1975, **19**, 1163–1179.

110 Y. Kobayashi, S. Tokishita and H. Yamamoto, Determination of Hansen Solubility Parameters of Ionic Liquids by Using Walden Plots, *Ind. Eng. Chem. Res.*, 2020, **59**, 14217–14223.

111 M. S. E. Houache, C. H. Yim, Z. Karkar and Y. Abu-Lebdeh, On the Current and Future Outlook of Battery Chemistries for Electric Vehicles—Mini Review, *Batteries*, 2022, **8**(7), 70.

112 C. Li, *et al.*, Perception of insight in the formation of solid electrolyte interphase, *Electrochim. Acta*, 2023, **468**, 143189.

113 X. Chen, N. Yao, B. S. Zeng and Q. Zhang, Ion–solvent chemistry in lithium battery electrolytes: From mono-solvent to multi-solvent complexes, *Fundam. Res.*, 2021, **1**, 393–398.

114 X. Q. Zhang, X. B. Cheng, X. Chen, C. Yan and Q. Zhang, Fluoroethylene Carbonate Additives to Render Uniform Li Deposits in Lithium Metal Batteries, *Adv. Funct. Mater.*, 2017, **27**(10), 1605989.